Reviewer 1

The manuscript reports the results of experimental burns over a rainfall transect of savanna where C4 grass represented from 35% to 99% of the standing biomass. The article reports and discuss results about the influence of standing biomass on fire residence time, production of HyPyC, and effect on the isotope disequilibrium induced by the combustion processes (SIDE). The authors found a negative correlation with the production of recalcitrant PyC (HyPyC) and a 13C in PyC compared to parent material. The hypotheses tested are extremely relevant both for the modeling of the impact of fires on C cycle and for reconstruction of past fire regimes. The experimental design is very innovative. The hypotheses tested were clearly stated in the introduction. There- fore I suggest the publication of this article in biogeoscience after some minor revision.

…Specific comments

Our comments are in bold

Line 8-9: please specify the meaning of distal and proximate fluxes in this context (is clarified in the text, but it may worth a clarification also in the abstract).

We have now introduced this clarification in the abstract. The text now reads: '…with each of these fluxes also partitioned into proximal (>125µm) likely to remain close to the site of burning, and distal (<125µm) likely to be transported from the site of burning.'

Line 12: 17: I completely with the authors on the wide range of residence time estimates. Nonetheless the authors report that: "some components of PyC appear to be susceptible to degradation on comparatively short timescales (Bird et al., 1999; Zimmermann et al., 2012) while some are resistant to degradation, remaining in soils and sediments for thousands to millions of years (Cope and Chaloner, 1980; Lehmann et al., 2008; Masiello and Druffel, 1998)." I am not sure whether this difference is due to the presence of components having different decomposition rates or rather can be attributed to the different methodologies adopted to estimate PyC decomposition (incubation vs observation).

While the use of different techniques does indeed lead to different results, it has become quite apparent over the years that the PyC continuum is also associated to a PyC degradation continuum (e.g. Kanaly and Harayama, 2000; McBeath and Smernick, 2009; Zimmermann et al., 2012).
In the text we include the statement above and make reference to our latest work, which is a compilation of the Pyrogenic Carbon Cycle addressing these very questions (Bird et al., 2015).

Bird, M. I., Wynn, J. G., Saiz G., Wurster C. M., and McBeath A.: The Pyrogenic Carbon Cycle, Annual Review of Earth and Planetary Sciences, 43, 2015.

Kanaly, R. A., & Harayama, S.: Biodegradation of high-molecular-weight polycyclic aromatic hydrocarbons by bacteria. Journal of bacteriology, 182, 2059-2067, 2000.

McBeath, A. V. and Smernik, R. J.: Variation in the degree of aromatic condensation of chars. Organic Geochemistry, 40, 1161-1168 2009.

Line 16-23: are these Kuhlbush (1996) and Masiello (1998) the most up to date articles on this topic?

We feel that the article by Kuhlbusch et al. (1996) needs to be cited in this context, as it is a seminal field-based experiment that has directly determined the initial allocation of PyC produced immediately after savanna burning. Moreover, and as indicated above, we also make reference to the most updated work covering these topics (Bird et al. 2015).

Page 15556: Line 10: In general were also reported the effect of being in a Tree (T) location or near a Grass (G location)?

The purpose of covering Tree (T) and Grass (G) locations was to encompass the widest possible range of spatial biomass (fuel) heterogeneity, which, as explained in another comment below, would minimise autocorrelation issues. Beyond the expected grass/woody biomass ratios (expressed in % grass biomass in newly named Table 2) it is unfortunately not possible to draw any sensible conclusions about their influence on PyC production, as they would just be based on two single observations per site.

Page 15159: The soot retrieved after cleaning the structure was it added to the >125 pool or < 125 or was it not measured? As it is specified later this is classified as distal, I suggest the authors report this also here for clarity. Also I would appreciate if they could discuss at which distance it is likely that fine particles are transported.

We have added the expression: 'This fraction was subsequently added to the distal (<125 μm) pool'. In addition, section 4.2 now contains a statement about the transport of fine PyC particles.

Page 15160: Line 16: Was all the non-HyPyC-C remaining after fire considered PyC? Was the hypotheses that part of the TEC was not altered by combustion discarded? I think that this is just a terminology issue, but it could worth to stress it in the text.

In the last paragraph of the introduction we acknowledge that there could still be some material non-thermally affected after the burns. The text reads: 'Here, we use the term PyC to describe all post-fire carbon, which in our experiments might also include non-thermally altered material'.
Coarse woody debris (CWD) was not considered due the small-scale experimental set-up. However, all the chosen locations and quadrats harvested for biomass quantification were studied as originally found, with

every residue left after the fire being accounted for (regardless of their degree of combustion).

Page 15161: Line 12-16: I did not find very clear why two different methods were used. Basically you estimated first the real bulk 13C content by measuring it (and I assume was somewhere in between -13 and -27) and then you measured the theoretical bulk 13C based on a two pool mixing model? Did the two measures agreed?

This is correct—the reviewer has understood the two methods that were used. We added a statement as to why this was done, and noted that the methods generally agreed.

Line 24-26: It is not clear to me against what the SIDE was regressed, i.e. what was the explanatory variable of the SIDE? From figure 4 it looks like they were regressed against grass biomass. I suggest the authors report it in the text as well.

The explanatory variable is now described in the text.

Line 27: of an F test, I would substitute with: "with an F test". Did the authors also tested the normality and constance of errors using the power model?

The text is now replaced as suggested by the reviewer. The normality of residuals was tested with Jarque-Bera test, and stats are reported in the figure.

Page 15162: This measure of fire residence time, is very interesting, it could worth to describe it in more in depth in the material section if it was created ad-hoc by the authors or cite the works if previously adopted, why was 100◦C chosen?

We have incorporated a brief description of this measure of fire residence time in M&M. We chose this temperature threshold on the basis of anecdotal evidence gathered during previous experimental fires conducted at these very ecosystems (Saiz et al, 2014). We observed a close parallelism between temperature and smoke emissions, which virtually ceased when temperature dropped round about 100 degrees.

Line 22: as it is reported in the figure the decrease is significant, I suggest the authors report it also in the text.

We have also added the significance of this relationship in the text.

Line 15: Why was the median used as a measure of central tendency instead of the mean? Were there many outliers?

With such a small sample size (n=16), it is difficult to say whether the distribution is normal. To be conservative, we used the median.

Figure 4: Since "The 13C of the CO2 was calculated by mass balance using the amount and isotopic composition of initial biomass and and the residual product of combustion", I was surprised that the uncertainty on the 13C of the CO2 was so little in fact this results from the sum of other measures (each having its own uncertainty usually higher than the one of CO2), therefore I would expect that the uncertainty would increase.

This is indeed a bit surprising. We note however, that the uncertainty was not calculated by propagating errors on the other estimates, but rather by statistics of the distribution of d13C of CO2.

Pag 15164: So if I understood correctly in nature high TCE correspond to short residence time fires, while you observed the opposite. Could this be an artifact of the chamber you installed?

We actually think that, under comparable environmental conditions, large biomass fires are likely to result in longer fire residence times compared to low (but continuous) biomass sites, if only because there is more material to be burnt. Moreover, in our experiment sites with the larger TCE contained a larger presence of woody biomass (Table 1), which would normally combust slower than the characteristically finer grassy biomass.

Pag 15165: Allocation of HyPyC produced during savanna fires: could the author discuss a bit deeper the mechanisms that regulate the relation between transport and residence of PyC in soil?

The discussion section (4.2) contains now a statement about the potential causes that may influence the transport and residence of newly produced PyC particles.

Page 15180: Figure 3: Was it taken into account that the part of the points where spatially correlated ? I mean that the points coming from the same area are likely to be spatially correlated, and could therefore be considered pseudoreplicates. This inconvenient could be solved by either using multiple variance anova, or mixed effect models. I think that r squared are not ideal to describe the fit of non-linear model (http://www.ncbi.nlm.nih.gov/pmc/articles/PMC2892436/)

We took the effort of spreading the location of the experimental fires across the natural ecosystems to minimise this effect. Furthermore, we point out in the text that, in tropical savannas, the abundance and $\delta^{13}C$ values of litter and standing biomass are quite heterogeneous at a local scale. This heterogeneity is largely controlled by the distribution of trees, and consequently we conducted duplicate burns at locations at half crown distance from trees ('Tree'; T locations), and at two additional locations remote from trees ('Grass'; G locations). Taking these factors into account, we were reasonably confident that we had likely encompassed the widest possible range of spatial heterogeneity, thus minimising autocorrelation issues.

We thank the reviewer for pointing out this common bias. We have now supplemented the degree of fitness (r^2) of the calculated equations with a Bayesian Information Criterion (BIC) as recommended by the suggested publication, so the reader can have more balanced information about how much these models could compare with others.

Reviewer 2

The manuscript by Saiz et al. describes a series of experimental burns in Australia in which they measured the isotopic composition of pyrogenic carbon emitted and de- posited after the fire. The authors show that relative to the isotopic composition of the carbon in the original fuels, the composition of pyrogenic carbon is more depleted, which is consistent with products from trees and shrubs ending up preferentially in this recalcitrant carbon pool. It is also more consistent with C4 grass biomass combusting more efficiently. Pyrogenic carbon emissions from fires (including savanna fires) are highly uncertain and poorly constrained by measurements. Hence, this study presents and exciting opportunity to look directly at the production and isotopic composition of pyrogenic carbon from savanna fires. Measuring fire-derived PyC is particularly challenging and this study presents an innovative approach, which is an important contribution to our capabilities of directly measuring PyC from savanna fires. While the study address issues that are of great importance for the field, hence contributing to our knowledge and understanding of PyC production and composition during savanna fires, there are a couple of aspects of the methods and results that are not very clearly explained in the current version of the manuscript. Overall the introduction is comprehensive, well balanced and provides a clear motivation for the study in terms of implications for the carbon cycle, interpretation of the origin of soil carbon pools using isotopes, and aerosols. The methods look to be state-of-the-art and are described in a robust way. The methods and results are logically presented, although as described below, some additional information would be helpful to the reader. In the discussion, the size of the impact of the isotopic disequilibrium presented by the authors here is likely to be an upper bound because some of the depleted pyrogenic carbon would be expected to decompose in subsequent years, lowering the instantaneous effect measured immediately after fire. Over all the paper presents new observations collected in a careful and quantitative manner that are relevant for fields of paleoecology and studies of atmospheric composition. In this context, the paper is likely to be relevant and of interest to readers of Biogeosciences. In the opinion of this reviewer, the paper may be suited for publication after consideration of the comments below.

...Specific comments

Our comments are in bold

The authors may wish to provide more motivation for isolating a HyPyC component of the pyrogenic carbon and description of their approach for measuring HyPyC. While the difference between the HyPyC and PyC pools is based on the chemical definition, the implications and meaning of this distinction are not very clear.

We have used the last paragraph of the introduction to further stress the importance of not just focusing on total PyC but in its most recalcitrant component as well (HyPyC).

In the results section 3.1. (Production of PyC during savanna burning) – PyC is only mentioned once, whereas the rest of the text is focused on HyPyC.
This section is now expanded a bit more and makes use of the concept of combustion completeness as suggested by the reviewer later on. Now the contribution of PyC is also better balanced in the first section of the discussion (4.1), as we have discussed our results in light of previous studies.

When the SIDE effects are discussed though, the authors note that the significance of SIDE during burning is more pronounced when considering the PyC produced by the fires than when considering the HyPyC component alone. What mechanisms contributing to this difference?
Indeed, the significance of SIDE is more pronounced when the PyC pool is considered as a whole. In section 3.2 we include the statistics for both the proximal and distal fluxes. For the distal fraction the difference between SIDE of PyC vs HyPyC is not significant ($p=0.25$), while it is significant for the proximal fraction ($p<0.01$). In the discussion section (4.3) we argue that the observed patterns highlight the importance of SIDE for the more labile or semi-labile components of the PyC flux, into which C4-derived PyC may be preferentially partitioned. Whereas the significance of SIDE is less pronounced in the more stable pool of PyC flux, into which C3-derived PyC may be preferentially partitioned. This is thus, the mechanism that may account for the PyC-HyPyC differences.

Another aspect discussed in the paper is the partitioning of PyC and HyPyC into distal and proximal fluxes, based on particles size separation of greater (distal flux) and smaller (proximal flux) than125 micrometers. More information on why 125-micrometer threshold is used as the separation point between the two size fractions is needed.
Section 2.2.2 in M&M, contains a statement justifying our choice, further supported with two references. The text reads: 'This mesh size was chosen to conform to standard dimensions used to differentiate between micro- and macro-charcoal in palynological studies, e.g. Blackford (2000); Haberle (2005)'.

Blackford, J.: Charcoal fragments in surface samples following a fire and the implications for interpretation of subfossil charcoal data, Palaeogeography, palaeoclimatology, palaeoecology, 164, 33-42, 2000.

Haberle, S.: A 23,000-yr pollen record from Lake Euramoo, Wet Tropics of NE Queensland, Australia, Quaternary Research, 64, 343-356, 2005.

The authors conclude the manuscripts by discussing the implications of this study for the 13C composition and interpretation of soil organic carbon (SOC). However, the concept and importance of SOC and its isotopic composition are barely mentioned in the rest of the paper – one sentence in the abstract and one in the introduction. The SOC topic needs further emphasis, and it is more suitable to move this section to the discussion rather than the conclusions.
We agree that some reorganization of the paper, as well as some emphasis on these points, makes this a stronger contribution. We moved the discussion of implications for SOC to a section in the discussion. We then

made the conclusions section a simple summary of the main points of the paper.

Figure 1 is complicated and includes 5 panels and a table. It would be easier for the reader if the lat/lon information and site information were contained in a separate stand-alone table. This would also give the authors an opportunity to write out the full site names for all the sites, some of which are not provided in the text. It would also allow the reader to more easily see the pictures of the individual sites, which are now relatively small. It would also be helpful if the map of the study area is bigger with more clearly defined vegetation cover (maybe overlay vegetation cover layer on top of the image of Northern Australia).

We have split former Figure 1 into two new figures (Fig. 1 and Fig. 2) and a new table (Table 1) according to his/her suggestions. We did attempt to overlay a reputable land cover map on new Figure 1, but as a result of the non-unified nomenclature used in vegetation classification in different tropical/subptropical systems (i.e Australia, Africa and South America), we felt that rather than helping the reader to extract more information, it was actually making things more difficult. In any case, a combination of Figure 1, 2 and Table 1, should provide sufficient information for a good comprehension of our work.

In the calculations and modeling, why assume mean isotope values from the literature for C4 grass biomass? Why not use C4 grass values measured from the individual field sites?

We used two methods to estimate the isotopic composition of total biomass, one based on assumptions from the literature, and the other based on measured values (see text). The two approaches generally agree (see response to reviewer 1 comments). We have added some text to address as similar comment in response to reviewer 1.

How robust is the SIDE effect computed in Figure 5d as a function of grass biomass with respect to these assumed values?

Because there is good agreement between the two methods of estimating $d^{13}C$ of biomass, we feel the analysis in the newly named Figure 6d is robust, and includes an analysis of errors associated with these estimates.

In the fire carbon cycle literature, combustion completeness (the amount of fuels consumed relative to their starting abundance) is used as a measure to analyze emission factors and other processes. The authors may wish to add a sentence or two about these results to the first paragraph of the results, and perhaps add a column for it to Table 1.

We have added the concept of combustion completeness in the first paragraph of the results, and have provided the median [range] for all fires. In our study, this measure is reciprocal to that of production of PyC relative to TCE, which is already shown in newly named Table 2.

The hypothesis that biomass from C3 vegetation is preferentially integrated into the pyrogenic fraction, contributing the observed disequilibria is an interesting

one. Is it contradicted by the individual site results from MIT grassland sites that also show a strong disequilibrium effect, yet from the site pictures, no trees or shrubs appear to be influencing the composition for the grassland sites at this location?
MIT sites were mainly composed of an axylale stratum (grass and herbs) as the newly named Table 2 shows (99.8-97.5 % grass biomass). However, it was still possible to observe some shrubs/small trees in isolated spots at the landscape level. We also noticed the occurrence of sparse *Acacia sp.* seedlings underneath the grass stratum that would likely be combusted in subsequent fires.

For the mass balance d13C estimate, please clarify it is really the isotopic composition of CO2 and other trace gases (CO, CH4, etc) which may add up to 3-5% or more of the total combusted loss.
We have added this clarification in the methods section.

Page 15166. The estimate of the global disequilibrium from pyrogenic fractionation (0.75 Pg C per mil) is really an upper bound, in the opinion of this reviewer, because it does not take into decomposition of some or most of the depleted PYC material in the months and years after fire. This has to be a lot, because the pre-fire HyPyC is less than half the post-fire HyPyC on average from Table 1, the FRT is ~ 2 years, and it's difficult to imagine erosion is a dominant pathway at these relatively flat and dry sites.
We have added this clarification in the text.

Minor comments:
Page 15158: Line 15 –Define TOC – acronym is used for the first time.
The acronym is now defined.

Page 151159: Line 3-4 – The authors mentioned they weighted samples pre- and post-drying to determine fuel moisture. It would be interesting to know the results, whether or not the moisture was high/low/variable, and if it could have any possible effects on the PyC production.
Regrettably, we were only able to retrieve fresh biomass weights for about half of the experimental burns. Therefore, we could not assess the potential effect of fuel moisture on PyC production in a robust manner. The experiments for which we could accurately calculate fuel moisture contents showed that they were all consistently low (<12% on a dry basis) showing very small variability among them. This result is hardly surprising as fires were purposely chosen to occur on days with no prior recorded rainfall for at least two weeks and at times coincident with maximum daily temperatures. Besides, fires took place late in the dry season, which in these ecosystems is characterized by the presence of senesced vegetation.

There is a typo or mis-formed sentence on page 15159 between lines 20 and 25 "evaporator remove the liquid"
We have corrected this. The text now reads: 'the soot retrieved after cleaning the structure with the water/methanol solution was placed in a rotary evaporator to remove the liquid phase'.

Page 15160 : Line7 – Write out Mo – molybdenum is used for the first time. Section 4.3.
The entire molybdenum word is now used.

Page 15165 Line 18-19: "Values consistent with relative 13C depletion of PyC in savanna fires" – citations?
The work by Krull et al. (2003) is now cited.

General comment - please consider including SIDE values in Table 2
We considered this, but these are relatively simple subtraction calculations. To minimize complexity of the table, we leave these calculations to the reader.

Pyrogenic carbon from tropical savanna burning: production and stable isotope composition

Gustavo Saiz[1,2*], Jonathan G. Wynn[3], Christopher M. Wurster[1], Iain Goodrick[1], Paul N. Nelson[1], Michael I. Bird[1]

[1]College of Science, Technology and Engineering and Centre for Tropical Environmental and Sustainability Science, James Cook University, P.O. Box 6811, Cairns, Queensland, 4870, Australia

[2]current address: Institute of Meteorology and Climate Research, Karlsruhe Institute of Technology, Garmisch-Partenkirchen, Germany

[3]School of Geosciences, University of South Florida, 4202 East Fowler Ave, NES107, Tampa, Florida 33620, USA

*corresponding author – email: gustavo.saiz@kit.edu; Ph: +49 (0) 8821 183 288

Deleted: School of Earth and Environmental Science

Keywords: carbon isotopes, savanna, biomass burning, black carbon, pyrogenic carbon, hydrogen pyrolysis

Abstract

Widespread burning of mixed tree-grass ecosystems represents the major natural locus of pyrogenic carbon (PyC) production. PyC is a significant, pervasive, and yet poorly understood 'slow-cycling' form of carbon present in the atmosphere, hydrosphere, soils and sediments. We conducted sixteen experimental burns on a rainfall transect through northern Australian savannas with C_4 grasses ranging from 35 to 99% of total biomass. Residues from each fire were partitioned into PyC and further into recalcitrant (HyPyC) components, with each of these fluxes also partitioned into proximal (>125µm) likely to remain close to the site of burning, and distal (<125µm) likely to be transported from the site of burning. The median [range] PyC production across all burns was 16.0 [11.5]% of total carbon exposed (TCE), with HyPyC accounting for 2.5 [4.9]% of TCE. Both PyC and HyPyC were dominantly partitioned into the proximal flux. Production of HyPyC was strongly related to fire residence time, with shorter duration fires resulting in higher HyPyC yields. The carbon isotope ($\delta^{13}C$) compositions of PyC and HyPyC were generally lower by 1-3‰ relative to the original biomass, with marked depletion up to 7‰ for grasslands dominated by C_4 biomass. $\delta^{13}C$ values of CO_2 produced by combustion was computed by mass balance and ranged from ~0.4 to 1.3‰. The depletion of ^{13}C in PyC and HyPyC relative to the original biomass has significant implications for the interpretation of $\delta^{13}C$ values of savanna soil organic carbon and of ancient PyC preserved in the geologic record, as well as for global ^{13}C isotopic disequilibria calculations.

Deleted: in

Deleted: fluxes.

Deleted: , likely to remain (initially) close to the site of production

Deleted: and

1 Introduction

Pyrogenic carbon (PyC) describes carbon (C) in a continuum of thermally altered materials produced by incomplete biomass combustion and ranging from partly-charred organic matter to condensed polyaromatic compounds (Hammes et al., 2007; Masiello, 2004). Components of the PyC continuum have been referred to by a variety of other terms, including soot, char and black carbon (Bird and Gröcke, 1997; Seiler and Crutzen, 1980). This range of names reflects the compositional complexity of PyC and the wide array of analytical methods employed for its quantification (Hammes et al., 2007; Ascough et al., 2009). While there is wide recognition of the large relevance of PyC affecting environmental processes (Bird et al., 1999; Cope and Chaloner, 1980; Lehmann et al., 2008; Zimmermann et al., 2012), it remains a poorly understood component of the global carbon cycle (6). Estimates of global PyC production rates have varied considerably since first reported (Seiler and Crutzen, 1980). The difficulty in establishing a reliable estimate of PyC production rates arises from the range of definitions used for PyC, usually operationally defined by the analytical technique used, and also by widely divergent experimentally-derived estimates of PyC production (Forbes et al., 2006). Calculations of the size of a global atmospheric C sink to PyC are also complicated because some components of PyC appear to be susceptible to degradation on comparatively short timescales (Bird et al., 1999; Zimmermann et al., 2012) while some are resistant to degradation, remaining in soils and sediments for thousands to millions of years (Cope and Chaloner, 1980; Lehmann et al., 2008; Masiello and Druffel, 1998). While the use of different techniques does indeed lead to different results, it has become quite apparent over the years that the PyC continuum is also associated to a PyC degradation continuum (Bird et al., 2015).

Of the total PyC produced by biomass burning, it has been estimated that >90% remains (initially) close to the site of production and <10% is emitted to the atmosphere as aerosols (Kuhlbusch et al., 1996), with much of the PyC emitted to the atmosphere being ultimately deposited in the oceans (Bird et al., 2015). PyC that remains on the ground will potentially (i) be re-combusted in subsequent fire events (Saiz et al., 2014; Santín et al., 2013) (ii) be re-mineralized by biotic/abiotic processes (Saiz et al., 2014; Santín et al., 2013; Zimmerman, 2010; Zimmermann et al., 2012), (iii) be remobilized by bioturbation, wind or water in either particulate (Major et al., 2010; Rumpel et al., 2006) or dissolved form (Dittmar, 2008; Dittmar et al., 2012) and/or (iv) accumulate in the soil organic carbon (SOC) pool (Lehmann et al., 2008).

With fire return intervals of 5 years or less (Furley et al., 2008), tropical savannas are major loci of global annual PyC production. Forbes et al. (2006) estimated the annual PyC production rate from savanna fires to be 4-40 Tg yr^{-1} (of a global total of 50-270 Tg yr^{-1}), assuming 1-2% of carbon exposed to fires was converted to PyC. Van der Werf et al. (2010) estimated that 39% of a total of 2.1 Tg yr^{-1} PyC emissions to the atmosphere derived from the burning of tropical savannas and grasslands (including extra-tropical grasslands; http://www.falw.vu/~gwerf/GFED/GFED3/tables/emis_BC_absolute.txt), whereas, Bond et al. (2004) estimated savanna burning at 51% of total 'open-burning' emissions.

In tropical savannas, woody vegetation uses the C_3 photosynthetic pathway ($\delta^{13}C$ < -24‰), whereas the grasses primarily use the C_4 photosynthetic pathway ($\delta^{13}C$ values > -15‰) (O'Leary, 1988). Randerson et al. (2005) estimated that 31% of global fire emissions have a C_4 origin and that 20% of total C_4 biomass returns to the

Deleted: . M

Deleted: is

Deleted:

Deleted: and may comprise 12-31% of marine sedimentary organic C (Masiello and Druffel, 1998)

atmosphere each year as a result of fire. The production of PyC from C_3 biomass generally has little impact on the $\delta^{13}C$ of the PyC relative to the precursor biomass (< ~1‰; Krull et al., 2003; Das et al., 2010). However, Krull et al. (2003) found that $\delta^{13}C$ values of PyC from C_4 grasses were 1.5-5‰ lower than precursor biomass. Das et al. (2010) also reported PyC products with $\delta^{13}C$ values lower than original biomass, but noted a difference between 'smoke' ($\delta^{13}C$ value lower by 0.5-7.2‰, species dependent), and 'ash' (generally lower by up to 3.5‰). Therefore, while $\delta^{13}C$ values provide a useful tracer of the fate of tree and grass-derived PyC both during and after formation, the robust interpretation of $\delta^{13}C$ values requires a more nuanced understanding of the processes controlling fractionation effects.

At the global scale, models of terrestrial ^{13}C discrimination suggest about one quarter of the gross primary productivity (GPP) of the terrestrial biosphere is attributable to the C_4 photosynthetic pathway (Lloyd and Farquhar, 1994; Still et al., 2003). In contrast, recent work has suggested the fraction of C_4-derived biomass in SOC in savanna systems is much lower than GPP estimates would imply, partly due to C_4-derived C decomposing faster than C_3-derived C in the soil (Wynn and Bird, 2007; Wynn et al., 2006). However, it is also plausible that during savanna burning (i) C_4 carbon is preferentially combusted relative to C_3 woody biomass and/or (ii) C_4 biomass produces finer PyC particles than C_3 woody biomass, and thus C_4-derived PyC is more likely to be exported by wind, leading to a relative accumulation of C_3-derived PyC at the site of burning (and ultimately in the soil), with C_4-derived PyC preferentially accumulating in sites remote to burning and particularly in lacustrine sediments and the ocean (Bird and Cali, 1998). Differences between the $\delta^{13}C$ values of C released to the atmosphere vs. $\delta^{13}C$ values of the C as it was fixed, or vs. the

$\delta^{13}C$ value of the SOC pool, are referred to as 'isotopic disequilibria' in mass balance models of atmospheric CO_2 (Alden et al., 2010; Enting et al., 1995). In savannas, large disequilibria are largely due to differences in the residence time of C_3 and C_4 biomass (Randerson et al., 2005; Ciais et al., 1999; Ciais et al., 2005; Buchmann and Ehleringer, 1998).

Quantification of the contribution of savanna fires to terrestrial isotopic disequilibrium due to potential differences in the residence times of C_3- and C_4-derived C in vegetation and soil, is important for (i) correctly interpreting soil and palaeosol carbon isotope data (Cerling et al., 2011), (ii) informing modelling studies that use variations in the CO_2 $\delta^{13}C$ record to apportion sources and sinks of CO_2 (Randerson et al., 2005; Ciais et al., 1999; Ciais et al., 2005), and (iii) enabling an assessment of physical redistribution biases that might complicate the interpretation of the $\delta^{13}C$ record of PyC in terrestrial, lacustrine and marine sedimentary records (Bird and Ascough, 2012).

In this paper we use a series of controlled field burning experiments in four savanna environments of northeastern Australia, where the strong climatic gradient exerts a major influence on vegetation structure existing across this large region (Table 1, Figs. 1-2). The experiments were designed to quantify the production and fate of PyC during savanna burning. Specifically, we seek to determine (i) the proportion of savanna biomass that is converted to PyC during burning, (ii) the distribution of this PyC between different size classes and (iii) the proportion of PyC between that fraction remaining on the ground and that exported as fine particulates during burning.

Our study takes advantage of controlled conditions, and a purpose-built field apparatus designed to determine the stocks and fluxes of PyC from fires occurring in a variety of savanna types (Fig. 3, see section 2.2). In addition, we used mass and carbon isotope balances to test the hypothesis that there is a 'savanna isotope disequilibrium effect' (SIDE) during burning, which leads to (i) an overall more negative $\delta^{13}C$ values for PyC produced in savanna fires due to the more complete combustion of C_4 biomass (and hence more positive $\delta^{13}C$ values for CO_2 of combustion produced in savanna fires), and (ii) an additional decrease in the $\delta^{13}C$ value of PyC remaining at the site of production, due to the preferential export of fine C_4-derived PyC.

Deleted: Fig. 2

Because PyC represents a continuum of materials of various degradabilities, we focus on the quantification of the refractory PyC component (HyPyC, polyaromatic ring number >7; see methods for full definition), likely to have at least a centennial residence time in the environment. Indeed, an accurate determination of the abundance and stable isotope composition of the HyPyC component formed in newly produced PyC is critical both for achieving an improved understanding of PyC dynamics, and for better interpreting records of biomass burning, climate and vegetation change in the past (Bird et al., 2015; Wurster et al., 2012). Here, we use the term PyC to describe all post-fire carbon, which in our experiments might also include non-thermally altered material.

2 Materials and Methods

2.1 Study sites

The study sites were located across four contrasting savanna-grassland ecosystems in Queensland (Australia). The sites extended from the drier inner region

to the more humid environments occurring near the northeast coast (Fig 1). The different climatic conditions prevailing at the various locations strongly influenced both the species and structural composition of these ecosystems. While there are many definitions of 'savanna' (Torello-Raventos et al., 2013; Domingues et al., 2010) the functional definition used for the purpose of this study is that of a biome consisting of a continuous graminoid component coexisting with woody plants at varying densities. The regional classification of vegetation was done according to Torello-Raventos et al. (2013). We chose a wide climatic range in order to provide the experiment with a broad spectrum of woody vs. grass biomass proportions (woody is equivalent to C_3 and grass to C_4). Indeed, there was a noticeable trend both in total biomass and in the relative contribution of woody (C_3) vegetation to the total biomass across the climatic gradient (Tables 1-2). The transect spanned dry Mitchell grasslands (site = MIT; MAP = 435mm) characterised by >97% C_4 grasses, to more humid tall savanna woodlands (site = DCR; MAP = 2050mm). The tall savanna woodlands exhibit a larger net contribution of 50-60% C_3 vegetation to the total biomass. While C_4 biomass was relatively constant across all sites, woody biomass increased with MAP (Fig. 2, Tables 1-2). Tree canopy cover was determined by means of site-specific allometric equations and visual estimates (Torello-Raventos et al., 2013; Domingues et al., 2010), and ranged from <5% for a site established in a heavily dominated grassland ecosystem (Mitchell grassland-MIT) to 55% for a tall savanna woodland occurring at about 20 km from the coast (Davies Creek National Park-DCR) (Fig 1).

Deleted: Table 1

Deleted: Fig. 1

Deleted: Table 1

The biomass present at all the fire experiment areas was mainly composed of a grass layer dominating with sparse *Eucalyptus* and *Acacia* tree seedlings with variable

amounts of coarse woody debris and leaf litter. The most abundant grass species were *Themeda australis, Imperata cylindrica and Heteropogon contortus*.

2.2 Field methods

2.2.1 Plot setup and pre-burn sampling

The experimental setup was designed to provide an estimate of initial total organic C, PyC abundance and $\delta^{13}C$ values, serving thus as reference to compare against post-burn samples. Burning experiments were carried out on a small scale [m^2], and were conceived to ensure the capture of all particulates to enable a full isotope and mass balance. As such, the experiments were not explicitly designed to simulate all characteristics of a 'natural' burn, but given the methodological issues surrounding all such techniques, the estimates of PyC production derived from this work are unlikely to be more uncertain than those obtained with other systems (cf. Forbes et al. (2006) for a review). Finally, we did not consider nor include burnt coarse woody debris, making the reasonable assumption that most PyC production in savanna fires occurs close to the ground from grass, litter, and shrubs (Randerson et al., 2005).

A total of four burning experiments were conducted at each of the four study areas, with specific assessments of both initial biomass and PyC inventory carried out before each burn. At a local scale the abundance and $\delta^{13}C$ values of litter and standing biomass are quite heterogeneous in tropical savannas. This heterogeneity is largely controlled by the distribution of trees, with lower average $\delta^{13}C$ values for litter and soil C around trees compared to grass dominated areas away from the influence of trees (Wynn et al., 2006; Saiz et al., 2012). Therefore, duplicate burns were conducted at locations at half crown distance from trees ('Tree'; T locations), while two

additional burns were also conducted remote from trees ('Grass'; G locations). Biomass was quantified in the near vicinity of each planned burn location by means of destructively collecting all aboveground plant material from two 1 m^2 census quadrats. In order to estimate PyC lying on the soil surface, each quadrat was subsequently vacuumed using a DC 23 Motorhead vacuum cleaner (Dyson Appliances Ltd., NSW, Australia). This task was systematically performed by the same user and over the same length of time across all burning experiments to allow for inter-comparison of results. Both the biomass and the vacuumed material were stored in separate labelled plastic bags. This sampling procedure was carried out in duplicate at each burning location, which resulted in a total of 8x1 m^2 census quadrats being sampled per studied site (Fig. 3).

Deleted: Fig. 2

2.2.2 Experimental burns

Four small-scale (1 m^2) burning experiments were conducted at each of the four study areas on sites with no recorded fires for two years during the late dry season of 2011. This period represents the maximum fuel load being available throughout the year as a result of the presence of senesced grasses that have already reached their full growth potential, and the fact that a number of tree species preferentially shed their leaves at this time. All the burns took place on days with no prior recorded rainfall for at least two weeks and shortly after midday, as this time generally corresponds to maximum daily temperature (T). This combination of factors results in optimum conditions for the occurrence and spread of fire in these ecosystems. At the time of the burns wind speeds were lower than 10 km h^{-1} in all cases, air T ranged from 24.2 to 40.0 °C, and relative humidity varied from 45 to 17 %.

A rectangular area of approximately 3x2 m was consistently left undisturbed at the centre of each planned fire. At this location, a purpose-built stainless steel structure was deployed to allow for both the assessment and containment of the experimental burning (Fig. 3). The final placement of the structure was chosen considering both the prevailing wind and topography with a view to strategically allocate an untouched area of vegetation (>1 m^2) over which the fire could be ignited promoting a natural progression of the flames towards the unit. Once the structure was positioned on the ground, a 10 m radius buffer zone was cleared to the ground (Fig. 3).

Deleted: Fig. 2

Deleted: Fig. 2

The structure consisted of a series of leaning panels made up of lightweight stainless steel, which was several times the volume occupied by the enclosed vegetation. The leaning panels provided extra volume for an optimal collection of smoke and airborne particles, with their lower sides positioned at 15 cm above ground-covering metal sheets to ensure a combustion with no artificial oxygen limitation. The front panel of the unit was vertical and was open in its lower section to allow the entrance of the fire. The structure was covered by an enclosed pyramid-like chamber culminating in an outlet to 15 cm diameter steel tube connected ultimately to a Romac 2042K particle extraction unit (0.755 m^3 s^{-1}, 2hp motor; Ron Mack, Perth, WA, Australia). The extractor unit was in operation during the entire course of the burn and was only disconnected after the cessation of any noticeable smouldering. A 125 µm stainless steel sieve was installed in the flow path at the outlet of chamber. This mesh size was chosen to conform to standard dimensions used to differentiate between micro- and macro-charcoal in palynological studies, *e.g.* Blackford (2000); Haberle (2005). Smaller particles contained in the airflow downstream of the first mesh were then subsampled and semi-quantitatively estimated using a particle

collector and a constant flow sampling pump (Quick Take 30, SKC Inc., Pennsylvania, USA).

Continuous air flow monitoring was performed on a vertical pipe positioned after the extractor unit by means of a calibrated 160S series 'S' type Pitot tube (Dwyer Instruments, Inc., Indiana, USA) connected to a Testo 435-4 multi-function instrument (Testo AG, Lenzkirch, Germany). Fire T was recorded by means of K-type wire thermocouples connected to a data logger (Simple Logger II L642, AEMC Instruments, USA) logging at 5 s intervals. The thermocouples were placed at the centre of the burned area at 0.02 m above the ground, and at the outlet of the chamber. Fire residence time was defined as the length of time that air T at the chimney's outlet exceeded 100ºC. This temperature threshold accounts for most of the particulate emissions derived from a flaming front, and it is also likely to encompass the majority of smouldering emissions in grass-dominated ecosystems.

Deleted: over which

The fire was allowed to burn the biomass contained within the unit without any external intervention. After the flames self-extinguished, the leaning side panels of the structure were lowered to the ground to minimise any lateral export of the burned material. Once the unit cooled down, any remaining stubble within the enclosed burnt was cut at ground level, and the same vacuum procedure employed on the two adjacent biomass quadrats was used again to determine total organic carbon (TOC) and PyC remaining on the soil surface. In order to quantify and analyse the fine soot produced during each burn, all the panels making up the structure were dismantled and thoroughly cleaned by manually brushing with a water/methanol 1:1 solution, with the resultant mixture being stored in a glass flask. Likewise, particulates collected on the steel mesh and in the particle collector were then retrieved and

carefully stored to subsequently weighed and analyzed as described in the laboratory methods below.

In summary, each of the four experimental burns at each of four sites along the climate transect resulted in the field collection of the following samples:

- 2 biomass (vegetation quadrats)
- 3 ground-vacuumed (2 vegetation quadrats + 1 burnt quadrat)
- 3 airborne particulate samples from the burnt quadrat (1 from the steel sieve >125 µm, 1 from the particle collector, and 1 from the soot adhered to the metal panels).

2.3 Laboratory methods

2.3.1 Initial preparations

Biomass collected from each unburned reference quadrat was weighed, dried at 60°C for five days and re-weighed to determine fuel moisture. This material was then sorted according to either grass (C_4) or woody biomass (*i.e.* tree/shrub leaves, twigs; C_3). The vacuumed material from each quadrat was also sorted, and any biomass fragments found were cleaned and added to the corresponding vegetation category (*i.e.* grass or woody). Thereafter these were weighed, recombined (keeping some aliquots separate for further testing) and milled. The samples vacuumed from the quadrats (both pre-burn and post-burn) were sieved to 2 mm and weighed. Separate aliquots were then size fractionated by wet sieving at 125 and 10 µm to conform with the definition of microcharcoal (10-125 µm; Haberle 2005). This procedure enables separate analysis of very fine <10 µm PC that is likely to be a major component of aerosol PC (Andreae and Merlet, 2001).

Deleted: a

In the case of airborne particles captured in the system, the following preparation procedures were conducted: (i) the coarse airborne particles collected at the 125 µm steel sieve positioned at the chamber outlet were flushed with a water/ methanol solution (1:1) and underwent the same wet fractionation procedure as described above; (ii) the particles that passed through the steel mesh (<125 µm) were wet-sieved to 10µm; and (iii) the soot retrieved after cleaning the structure with the water/methanol solution was placed in a rotary evaporator to remove the liquid phase, but no attempt was made to size separate this soot, as intense physical brushing may have significantly altered the 'natural' particle size distribution. This fraction was subsequently added to the distal (<125 µm) pool. In all cases presented above, the resultant fractions were subsequently freeze-dried, weighed and finely milled in preparation for further analyses.

Deleted: that was contained in a glass flask

2.3.2 Hydrogen Pyrolysis

Hydrogen Pyrolysis has been described in detail in a number of publications (e.g., Ascough et al., 2009; Meredith et al., 2012; Wurster et al., 2012, Wurster et al., 2013). The technique separates PyC in aromatic clusters with a ring size >7 (HyPyC = PyC that is likely to be resistant to environmental degradation) from other organic C and has been shown to perform well in characterizing PyC abundance in a range of environmental matrices (Meredith et al., 2012). Briefly, the solid samples were loaded with a molybdenum catalyst (~10% of dry weight) using an aqueous/methanol solution of ammonium dioxydithiomolybdate [$(NH_4)_2MoO_2S_2$]. Dried, catalyst loaded samples were placed in a reactor and pressurized with 150 bar H_2 under a sweep gas flow of 5 L min^{-1}, then heated at 300°C min^{-1} to 250 °C, then stepped at 8°C min^{-1} to a final hold T of 550°C for 2 minutes.

Deleted: Mo

Because the catalyst that is loaded undergoes weight loss during hydrogen pyrolysis, the abundance of carbon in the sample after hydrogen pyrolysis is determined relative to TOC (the mass of carbon after treatment / the mass of carbon loaded) and reported as %HyPyC/TOC or %HyPyC/Sample.

2.3.3 Carbon abundance and isotope composition

Carbon abundance and isotope composition of samples were determined using a Costech Elemental Analyzer (EA) fitted with a zero-blank auto-sampler coupled via a ConFloIV to a ThermoFinnigan DeltaV^{PLUS} mass spectrometer using Continuous-Flow Isotope Ratio Mass Spectrometry (EA-IRMS) at James Cook University's Cairns Analytical Unit. Stable isotope results are reported as per mil (‰) deviations from the VPDB reference standard scale for $\delta^{13}C$ values. Precisions (S.D.) on internal standards were better than ±0.2‰.

2.4 Calculations and Modelling

Measured quantities of TOC, PyC and HyPyC in each fraction were summed into two fluxes from each of the fires: "distal" and "proximal". 'Proximal' (likely to remain close to the site of burning) includes that collected from the surface after the fire in addition to the >125 µm fraction collected from the sieve. 'Distal' (likely to be transported from the site of burning) includes the <125 µm fraction collected from the stainless steel sieve, as well as that collected in the particle collector attached to the pump, and the soot cleaned from the apparatus.

The percent grass biomass at each site was estimated from the mass of separated grass and woody biomass collected from two plots adjacent to the burning apparatus. An estimate of the initial isotopic composition of the biomass ($\delta^{13}C_{biomass}$) was

Deleted: calculated

Deleted: The

determined by two methods. First a bulk sample of the biomass from the two vegetation plots was homogenized and its $\delta^{13}C$ value measured. Second, the separately summed masses of grass and woody vegetation were used to estimate the bulk isotopic composition, assuming values for C_3 woody biomass (-27.2‰) and for C_4 grass biomass (-13.1‰; values from Cerling et al., 1997). The estimated percent grass biomass values produced by these two methods agreed (linear regression r^2 = 0.88). The average of the two estimates is used as the central tendency while the range of values is used as an error in these estimates. The carbon isotopic composition of CO_2 and other trace gases produced by combustion for each of the fires was calculated by mass balance using the amount and isotopic composition of initial biomass and of the residual products of combustion (note that this mass difference calculation of CO_2 likely includes other carbonaceous trace gases such as CO and CH_4).

The value of SIDE can be expressed as an 'isodisequlibrium forcing coefficient' following the terminology of Alden et al. (2010), which is a difference between the $\delta^{13}C$ values of forward and reverse fluxes between two reservoirs. The values of SIDE were calculated for each of the component fluxes from the fires as the difference between the $\delta^{13}C$ value of the flux ($\delta^{13}C_{flux,}$ for example the distal HyPyC component, $\delta^{13}C_{flux} = \delta^{13}C_{distal\ HyPyC}$) and the initial $\delta^{13}C$ value of the biomass ($\delta^{13}C_{biomass}$). The values of SIDE from each of the four fluxes was regressed with respect to the estimate of percent grass biomass using the Matlab curve fitting toolbox with a power function. Significance of the power law curve fit was calculated as a *p*-value, which describes the probability with an F-test that the relationship is a better estimate than simply the mean value of SIDE. Confidence intervals for the curve fit equations were calculated

Deleted:

Formatted: Superscript

Formatted: Subscript

Formatted: Subscript

Deleted: of

at p =0.9. The distribution of residuals were tested for normality with a Jarque-Bera test.

The savanna isotopic disequilibrium flux ($D_{SIDE\_CO2} = F_{bur}(SIDE_{CO2})$, where F_{bur} is the flux of C from annual biomass burning) was calculated for global savanna environments using an estimate of the fraction of C_4 photosynthesis from Still et al. (2003). The calculated F_{bur} value for savannas was averaged over the period from 1997-2011 using the Global Fire Emissions Database (GFED; http://globalfiredata.org; van der Werf et al., 2010), clipped to the area where C_4 grasses > 1% (Still et al., 2003). The global distribution of the isotopic disequilibrium flux was calculated and plotted using Generic Mapping Tools (GMT; Wessel et al., 2013).

3 Results

3.1 Production of PyC during savanna burning

The total carbon exposed (TCE) to combustion showed a discernable pattern across the precipitation gradient, with higher potentially combustible C in standing biomass and surface litter at the more humid sites (Table 2, Fig. 2). The median [range] production of PyC and HyPyC was 16.0 [11.5]% and 2.5 [4.9]% of TCE across all experimental burns (Table 2). Similarly, the amount of total carbon combusted (TCC) defined as the difference between TCE and post fire carbon was used to calculate combustion completeness (described as TCC relative to TCE), and whose median [range] for all fires was 84.0 [11.5)%. The median [range] amount of HyPyC in the proximal component (>125µm) of the flux from the fires was 96.9 [14.1]% of the total HyPyC flux across all experimental burns. Fire residence time, defined as time over which air T at the chimney's outlet exceeded 100ºC, increased

Deleted: .

Deleted: Table 1

Deleted: Fig. 1

Deleted: Table 1

with TCE (Fig. 4), and thus with the proportion of woody biomass (Table 2). The proportion of TCE converted to HyPyC significantly decreased with initial TCE, and thus decreased with the proportion of woody biomass (Fig. 4; Table 2).

Deleted: Fig. 3
Deleted: Table 1
Deleted: Fig. 3
Deleted: Table 1

3.2 Isotopic disequilibria of proximal and distal fluxes of PyC and HyPyC

The values of SIDE were computed from $\delta^{13}C$ values shown in Table 3. When considering the PyC pool, the median [range] SIDE value of proximal PyC ($SIDE_{\mathbf{proximal}\text{-}PyC}$ -3.3 [4.2]‰; where $SIDE = \delta^{13}C_{flux} - \delta^{13}C_{biomass}$, with superscripts proximal or distal and PyC or HyPyC are relevant to the flux) was not significantly different from the median [range] SIDE value of distal PyC ($SIDE_{distal\text{-}PyC}$; -4.7 [6.3]‰; p = 0.737, Mann-Whitney U; Fig. 5). However, the median [range] SIDE value of proximal HyPyC ($SIDE_{proximal\text{-}HyPyC}$ -1.1 [5.3]‰ was significantly different from the median [range] SIDE value of distal HyPyC ($SIDE_{distal\text{-}HyPyC}$; -2.9 [8.0]‰; p = 0.024; Fig. 5). Comparing the two proximal fluxes, the median value of $SIDE_{proximal\text{-}PyC}$ was significantly different from the median value of $SIDE_{proximal\text{-}HyPyC}$ ($p < 0.001$ Fig. 5). The median value of $SIDE_{distal\text{-}PyC}$ was not significantly different from the median value of $SIDE_{distal\text{-}HyPyC}$ (p = 0.245; Fig. 5). The median [range] SIDE value of CO_2 of combustion ($SIDE_{CO2}$) was 0.61‰ [0.88‰] (Fig. 5).

Deleted: Table 2
Deleted: Fig. 4
Deleted: Fig. 4
Deleted: Fig. 4
Deleted: Fig. 4
Deleted: Fig. 4

Neither $SIDE_{proximal\text{-}PyC}$, nor $SIDE_{proximal\text{-}HyPyC}$ show a significant relationship to the initial proportion of C_4 biomass (p = 0.50; and p = 0.44, respectively; Fig. 6). However, $SIDE_{distal\text{-}PyC}$ shows a significant power-law relationship to the initial proportion of C_4 biomass ($SIDE_{distal\text{-}PyC} = -1.068 \times 10^{-5}$ (%grass)$^{2.862}$ – 0.661; R^2 = 0.789; p = 0.007), with values decreasing towards the C_4-dominated end of the vegetation gradient (Fig. 6). Similarly, $SIDE_{distal\text{-}HyPyC}$ was positively correlated with the initial proportion of C_4 biomass ($SIDE_{distal\text{-}HyPyC} = -3.243 \times 10^{-7}$ (%grass)$^{3.589}$ –

Deleted: Fig. 5
Deleted: Fig. 5

0.298; R^2 = 0.577; p = 0.094). $SIDE_{combustion\text{-}CO2}$ showed no significant relationship to the initial proportion of C_4 biomass (p = 0.99).

4 Discussion

4.1 Production of PyC across contrasting savanna environments

The proportion of biomass converted to PyC and HyPyC during the experimental burns varied across the range of savannas studied (Table 2, Fig. 4). The median PyC/ TCE conversion rate of 16.0% is in the upper range of values reported in previous studies, although those could have underestimated actual PyC conversion rates due to a combination of factors, which include the use of analytical techniques focusing only on recalcitrant PyC components, the non-inclusion of all PyC materials being produced, and the choice of experimental fires not being representative of typical wildfire conditions (Santín et al., in press). However, the observation that the relative amount of HyPyC produced in grass-dominated savannas was larger than in woody-biomass-dominated savannas runs counter to our initial assumption that anticipated that more woody biomass would promote the production of proportionally more HyPyC. Longer fire residence times were positively correlated with greater TCE, which resulted in less HyPyC being formed due to the opportunity for more complete combustion (Fig. 4). Indeed, incomplete combustion of biomass can mainly be ascribed to the combined effects of low combustion T, short fire residence times, and an overall lack of available oxygen (Loo and Koppejan, 2002).

Typically, low fire residence time is reported for fast moving fires characteristic of landscapes with abundant fine fuel, such as savannas (Hartford and Frandsen, 1992; Wright and Bailey, 1982). While fire residence time was shorter for the grass-dominated sites, maximum T was quite comparable across all the studied sites (Table

Deleted: savanna

Deleted: Table 1

Deleted: Fig. 3

Deleted: burns

Deleted: Fig. 3

Deleted: Table 1

2), and agrees well with results reported for savanna fires elsewhere (Miranda et al., 1993; Trollope, 1984). Therefore, the short-lived fires occurring in grass-dominated ecosystems may result in the production of proportionally more HyPyC (Table 2, Fig. 4). The median [range] production of HyPyC as a proportion of both TCE and TCC were 2.5 [4.9]% and 2.9 [5.9]% respectively. These figures compare well with estimates of 'black carbon' (charcoal) production for savanna and grassland fires reviewed by Forbes et al. (2006).

Deleted: Table 1

Deleted: Fig. 3

Deleted: total carbon combusted (

Deleted:),

Deleted: defined as the difference between TCE and post fire carbon,

4.2 Allocation of HyPyC produced during savanna fires

In order to better constrain the global PyC cycle, there is an obvious need for a deeper understanding of the factors controlling formation, translocation and mineralisation of PyC and its recalcitrant compounds, represented here by HyPyC (Bird et al., 2015; Conedera et al., 2009; Zimmermann et al., 2012). In this context, the partitioning of PyC between the proximal and distal fluxes, may have a strong influence on preservation potential (Thevenon et al., 2010). Blackford (2000) reports an order of magnitude decrease in the percentage of charred particles >125 µm observed at just 7 m from a recently burned area. In contrast, smaller size particles can be transported by wind up to thousands of kilometres, with this range largely depending on the particle size, height of the convection column and environmental conditions (Clark, 1988). The total amount of HyPyC contained in both fluxes varied across the burning experiments, but with most of the HyPyC in the proximal flux in all cases. The proportion of HyPyC in the proximal flux was very large in grass-dominated savannas (>96% of total HyPyC at MIT), compared to the proportion of HyPyC in the proximal flux in woody-biomass-dominated savannas (86-91% of total HyPyC at DCR). This also suggests that longer fire residence times not only result in a more complete combustion of biomass, they may also promote more effective

Deleted: C

Deleted: Hy

comminution and volatilisation of fuel into fine particles and gases. Such an effect was also observed by Kuhlbusch et al. (1996) who found burning experiments with the highest fuel loads showed the highest degree of C volatilisation.

4.3 Savanna isotope disequilibrium effects (SIDE)

In general, the calculated SIDE values are consistent with relative ^{13}C-depletion of PyC produced during savanna fires (Krull et al., 2003), with some significant distinctions between proximal and distal fluxes, as well as between the PyC and the HyPyC fluxes (Fig. 6). A relative ^{13}C-depletion is more consistently observed for the proximal PyC, with δ^{13}C values always lower than the original biomass. The δ^{13}C values of the proximal flux of HyPy C were also generally lower, with the exception of two fires (UND 3-4; Table 3, Fig. 5). The distal flux of PyC also had lower δ^{13}C values than the precursor biomass. The observation that PyC is relatively ^{13}C-depleted with respect to the original biomass across all sites, supports the hypothesis that, where woody (C_3) and grass (C_4) biomass are both present, the (C_4) grass biomass is preferentially combusted relative to (C_3) woody material, leaving PyC from woody biomass to contribute disproportionately to the PyC flux (*i.e.*, $SIDE_{PyC}$ values are negative). Also because the δ^{13}C values of PyC are relatively ^{13}C-depleted with respect to original biomass, mass balance dictates that the δ^{13}C values of CO_2 of combustion are relatively ^{13}C-enriched with respect to original biomass (*i.e.*, $SIDE_{CO2}$ values are positive, Fig. 5).

This differential fractionation between the products of combustion and original biomass may represent a significant contribution to the global carbon isotope disequilbrium terms used in ^{13}C double deconvolution models of atmospheric CO_2 (Alden et al., 2010; Ciais et al., 2005; Enting et al., 1995). The isodisequilibrium

Deleted: Fig. 5

Deleted: Table 2

Deleted: Fig. 4

Deleted: Fig. 4

forcing coefficient for biomass burning, here referred to as I_{bur}, is defined as the difference in the $d^{13}C$ value of CO_2 produced by biomass burning and the $d^{13}C$ value of CO_2 into biomass regrown after burning:

$$I_{bur} = (\delta^{13}C_{CO2\_bur} - \delta^{13}C_{CO2\_regrow\_bur}) \quad (1)$$

while the disequilibrium associated with this term (D_{bur} of Ciais et al. (2005) is:

$$D_{bur} = F_{bur}(I_{bur}) \quad (2)$$

where F_{bur} is the atmospheric source flux of CO_2 due to biomass burning.

However, as used in double deconvolution mass balance models, I_{bur} assumes no isotopic fractionation associated with combustion, *i.e.*, that the $\delta^{13}C$ value of CO_2 of combustion ($\delta^{13}C_{CO2\_bur}$) is equal to that of biomass burnt ($\delta^{13}C_{biomass\_bur}$). Because our results show that CO_2 of combustion is ^{13}C-enriched with respect to biomass burnt (by a $SIDE_{CO2}$ value of about 0.6‰), we can explicitly account for this during the calculation of I_{bur}:

$$I_{bur*} = (\delta^{13}C_{biomass\_bur} + SIDE_{CO2} - \delta^{13}C_{CO2\_regrow\_bur}) \quad (3)$$

An asterisk is used to indicate that the term accounts for fractionation during combustion. The total burning disequilibrium becomes:

$$D_{bur*} = F_{bur}(\delta^{13}C_{biomass\_bur} - \delta^{13}C_{biomass\_regrow\_bur}) + F_{bur}(SIDE_{CO2}) \quad (4)$$

$$D_{bur*} = D_{bur} + D_{SIDE\_CO2} \quad (5)$$

The first term is the disequilibrium as calculated by Ciais et al. (2005), and assumes no fractionation associated with combustion. The second term explicitly accounts for $SIDE_{CO2}$ associated with differential combustion of C_3 and C_4 biomass. The global value of D_{SIDE_CO2} is estimated in Figure 7, to have a global sum of about 0.75 Gt C

Deleted: Figure 6

yr^{-1} ‰. This value may be an upper bound for D_{SIDE} because some of the ^{13}C-depleted PyC may be mineralized after the fire, as was observed by Zimmermann et al. (2012).

Figure 5 shows that in both the proximal and distal fluxes, the significance of SIDE during burning is more pronounced when considering the PyC produced by the fires than when considering the HyPyC component alone. The observed patterns highlight the importance of SIDE for the more labile or semi-labile components of the PyC flux, into which C_4-derived PyC may be preferentially partitioned. Whereas the significance of SIDE is less pronounced in the more stable pool of PyC flux, into which C_3-derived PyC may be preferentially partitioned.

We used particle size separations of PyC fluxes to test the hypothesis that PyC remaining near to the site of production shows a more pronounced SIDE due to preferential export of C_4-derived PyC in the finer particle size fractions. While no significant trends are observed for the proximal fluxes of PyC (neither the total, nor HyPyC components), the relationship is significant for both distal PyC and for distal HyPyC (Fig. 6). These observations indicate that in grass-dominated environments, the preferential export of fine particle size fractions is likely to be dominated by low $\delta^{13}C$ components of PyC. Thus, the SIDE is more pronounced in grass-dominated fires, either because (a) the small amount of C_3-derived PyC flux in these systems is preferentially exported in the fine (soot) fraction of the distal component, or (b) compounds with low $\delta^{13}C$ values are preferentially exported to the fine fraction (Das et al., 2010; Krull et al., 2003). Krull et al. (2003) attributed this effect to the occlusion of protected ^{13}C-depleted compounds in phytoliths of C_4 grasses, and our results further suggest that ^{13}C-depleted compounds (*e.g.*, lipids, lignins or phytoliths) may be preserved in PyC (O'Malley et al., 1997), being preferentially exported as

Formatted: Subscript
Formatted: Superscript
Deleted: Figure 4
Deleted: Fig. 5

607 highly condensed aromatic structures in the fine soot components of natural fires.
608 Another significant contributor to SIDE may also be the plant methoxyl pool, which is
609 extremely depleted in ^{13}C (~-29‰ in leaves relative to bulk biomass) and comprises
610 about 2.5% of plant biomass (Keppler et al., 2004). Moreover, the same authors report
611 that the fractionation associated with the methoxyl-groups may be further enhanced
612 during their conversion to volatile compounds (i.e. through burning), which could also
613 contribute to the low $\delta^{13}C$ values we observed in the soot fraction. Nonetheless, we
614 cannot rule out the possibility that a significant proportion of this 'soot' component
615 may derive from the small amount of C_3 biomass present, even in C4 dominated
616 ecosystems.

617 The small-scale experimental set-up used here did not consider coarse woody
618 debris (CWD), which is common in most savanna environments and may burn along
619 with other biomass on the ground. As this material is exclusively composed of C_3
620 biomass, the inclusion of PyC from CWD would likely increase the contribution of
621 proximal PyC to the total flux, further enhancing the SIDE on SOC $\delta^{13}C$ (Bird and
622 Pousai, 1997; Wynn and Bird, 2008).

623 **4.4 Implications of SIDE**

624 The calculation of the global SIDE 'disequilibrium flux' (Fig. 7) reinforces the
625 conclusion that the effects of SIDE during savanna burning are most pronounced in
626 grass-dominated savannas, where C_4 plants are the most significant fraction of
627 biomass. Scaling these trends up to the global scale indicates a significant SIDE
628 forcing for the savanna biome, which may contribute to a ^{13}C disequilibrium flux on
629 the order of 0.75 Gt C yr^{-1} ‰, a value which is of significant magnitude in
630 comparison to other ^{13}C disequilibrium fluxes used in mass balance models (Ciais et

Formatted: Font:Bold
Formatted: Indent: First line: 0 cm
Formatted: Font:Bold
Moved (insertion) [2]
Deleted: Fig. 6

al., 2005). This ^{13}C-disequilibrium flux ($D_{SIDE\ CO2}$) accounts for isotope fractionation associated with differential combustion of C_3 and C_4 biomass, which is otherwise not explicitly accounted for, and would contribute to the total biomass burning isotopic disequilibrium (D_{bur}) caused by regrowth of ecosystems after fire (1.66 Gt C yr^{-1} ‰; Ciais et al.; 2005).

Because grass-dominated savannas show high SIDE for PyC, the implication is that SOC in savannas with frequent grass-dominated fires will become increasingly ^{13}C-depleted, as the stable components of PyC accumulate in the soil over time. This observation is consistent with studies of SOC at large spatial scales; for example where grass-dominated Mitchell grasslands show lower δ^{13}C values of surface SOC (ca. -16‰) than is typical of C_4 biomass (ca. -12‰) (Bird and Pousai, 1997; Wynn and Bird, 2008), and agrees well with findings by Dümig et al. (2013) which indicate both the presence of charred grass residues and accumulation of alkyl C in soil fractions as the most likely contributors to the observed decreasing δ^{13}C values from grass biomass to C_4-derived surface SOC. Such a conclusion has implications for interpretation of paleorecords derived from ancient SOC or its by-products in sedimentary records, which may be biased towards ^{13}C-depleted values by this SIDE during savanna burning.

Moved (insertion) [1]

5 Conclusions

The production of PyC and HyPyC was quantified in sixteen experimental fires conducted along a transect of sites in northern Australian savannas. The residues after burning were partitioned into proximal and distal fluxes, each measured for their PyC and HyPyC contents and the carbon isotope composition of each component. The

Deleted: were observed during

Deleted:

Deleted: of

Deleted: the fire

Deleted: ic

production of PyC across all experimental burns ranges from 11.6 to 23.1% of TCE. TCE is positively correlated with fire residence time, and increasing fire residence time reduces the proportion of HyPyC produced due to the opportunity for more complete combustion. Thus, the short-lived fires occurring in grass-dominated ecosystems result in the production of proportionally more HyPyC compared to woodier-dominated savannas. The median [range] production of HyPyC as a proportion of both TCE and TCC across all experimental burns were 2.5 [4.9]% and 2.9 [5.9]% respectively. These figures are in good agreement with other estimates of 'black carbon' (charcoal) production for savanna and grassland fires (Forbes et al., 2006). The relative amount of HyPyC in the proximal flux is significantly larger in grass-dominated savannas (up to >99%) compared to that observed in woodier savannas (>86%). This is a significant observation as these two fluxes are likely to have different preservation potentials. The Savanna Isotope Disequilibrium Effect (SIDE, difference in carbon isotopic composition between grass biomass and pyrogenic carbon components) was highest at sites with the greatest proportion of grass biomass although this trend was only observed for the distal flux of fine-grained material (<125µm). Scaling the SIDE values observed here to the global savanna biome suggests that the SIDE effect contributes a significant $\Delta^{13}C$-disequilibrium flux to the global mass balance of $\Delta^{13}C$ exchange between the atmosphere and other reservoirs (Ciais et al., 2005). The observation that SIDE increases with increasing grass biomass also suggests that frequently burned savannas are subject to depletion of $\Delta^{13}C$ in the pyrogenic products. As the PyC produced by savanna fires accumulates, either in situ, or distally, the SIDE effect produces soil or sedimentary organic carbon with $\delta^{13}C$ values which are relatively $\Delta^{13}C$-depleted with respect to the original biomass. This effect may have significant implications for the interpretation of stable

Deleted: h

Formatted: Superscript

Formatted: Superscript

Formatted: Superscript

Formatted: Superscript

carbon isotopic composition of paleorecords which are based wholly or in part on PyC.

Author contribution

GS, JW, IG and MB designed the experiment. GS and IG carried out the fieldwork and conducted laboratory analyses. JW developed the model and performed simulations. GS, JW and MB prepared the manuscript with contributions from all co-authors.

Acknowledgments

This work was supported by Australia Research Council Grants DP1096586 and FF0883221. We gratefully acknowledge Queensland Parks and Wildlife staff for access to sites at Undara and Davies Creek. We are also thankful to the Australian Wildlife Conservancy Society for allowing access and permits to undertake research at the Brooklyn Sanctuary site, and the generous farmer who granted us permission to work in his property near Corfield (MIT site).

References

Alden, C. B., Miller, J. B., and White, J. W. C.: Can bottom-up ocean CO2 fluxes be reconciled with atmospheric 13C observations?, Tellus B, 62, 369-388, 2010.

Andreae, M. O., and Merlet, P.: Emission of trace gases and aerosols from biomass burning, Global Biogeochem. Cycles, 15, 955–966, 2001.

Ascough, P. L., Bird, M. I., Brock, F., Higham, T. F. G., Meredith, W., Snape, C. E., and Vane, C. H.: Hydropyrolysis as a new tool for radiocarbon pre-treatment and the quantification of black carbon., Quaternary Geochronology, 4, 140-147, 2009.

Moved up [2]: The calculation of the global SIDE 'disequilibrium flux' (Fig. 6) reinforces the conclusion that the effects of SIDE during savanna burning are most pronounced in grass-dominated savannas, where C_4 plants are the most significant fraction of biomass. Scaling these trends up to the global scale indicates a significant SIDE forcing for the savanna biome, which may contribute to a ^{13}C disequilibrium flux on the order of 0.75 Gt C yr^{-1} ‰, a value which is of significant magnitude in comparison to other ^{13}C disequilibrium fluxes used in mass balance models (Ciais et al., 2005). This ^{13}C-disequilibrium flux (D_{SIDE_CO2}) accounts for isotope fractionation associated with differential combustion of C_3 and C_4 biomass, which is otherwise not explicitly accounted for, and would contribute to the total biomass burning isotopic disequilibrium (D_{bur}) caused by regrowth of ecosystems after fire (1.66 Gt C yr^{-1} ‰; Ciais et al.; 2005).

Deleted: .

Moved up [1]: Because grass-dominated savannas show high SIDE for PyC, the implication is that SOC in savannas with frequent grass-dominated fires will become increasingly ^{13}C-depleted, as the stable components of PyC accumulate in the soil over time. This observation is consistent with studies of SOC at large spatial scales; for example where grass-dominated Mitchell grasslands show lower $\delta^{13}C$ values of surface SOC (ca. -16‰) than is typical of C_4 biomass (ca. -12‰) (Bird and Pousai, 1997; Wynn and Bird, 2008), and agrees well with findings by Dümig et al. (2013) which indicate both the presence of charred grass residues and accumulation of alkyl C in soil fractions as the most likely contributors to the observed decreasing $\delta^{13}C$ values from grass biomass to C_4-derived surface SOC. Such a conclusion has implications for interpretation of paleorecords derived from ancient SOC or its by-products in sedimentary records, which may be biased towards ^{13}C-depleted values by this SIDE during savanna burning.

Deleted: r

Deleted: NP

Deleted: .

762 Bird, M. I., and Gröcke, D. R.: Determination of the abundance and carbon isotope
763 composition of elemental carbon in sediments, Geochimica et Cosmochimica
764 Acta, 61, 3413-3423, 1997.
765 Bird, M. I., and Pousai, P.: Variations of δ13C in the surface soil organic carbon
766 pool, Global Biogeochem. Cycles, 11, 313–322, 1997.
767 Bird, M. I., and Cali, J. A.: A million-year record of fire in sub-Saharan Africa,
768 Nature, 394, 767-769, 1998.
769 Bird, M. I., Moyo, C., Veenendaal, E. M., Lloyd, J., and Frost, P.: Stability of
770 elemental carbon in a savanna soil, Global Biogeochemical Cycles, 13, 923-
771 932, 1999.
772 Bird, M. I., and Ascough, P. L.: Isotopes in pyrogenic carbon: A review, Organic
773 Geochemistry, 42, 1529-1539, 2012.
774 Bird, M. I., Wynn, J. G., Saiz G., Wurster C. M., and McBeath A.: The Pyrogenic
775 Carbon Cycle, Annual Review of Earth and Planetary Sciences, 43, 2015.
776 Blackford, J.: Charcoal fragments in surface samples following a fire and the
777 implications for interpretation of subfossil charcoal data, Palaeogeography,
778 palaeoclimatology, palaeoecology, 164, 33-42, 2000.
779 Bond, T. C., Streets, D. G., Yarber, K. F., Nelson, S. M., Woo, J. H., and Klimont, Z.: A
780 technology-based global inventory of black and organic carbon emissions
781 from combustion, Journal of Geophysical Research, 109, D14203, 2004.
782 Buchmann, N., and Ehleringer, J. R.: CO2 concentration profiles, and carbon and
783 oxygen isotopes in C3 and C4 crop canopies, Agricultural and Forest
784 Meteorology, 89, 45-58, 1998.
785 Cerling, T. E., Harris, J. M., MacFadden, B. J., Leakey, M. G., Quade, J., Eisenmann, V.,
786 and Ehleringer, J. R.: Global vegetation change through the Miocene/Pliocene
787 boundary, Nature, 389, 153-158, 1997.
788 Cerling, T. E., Wynn, J. G., Andanje, S. A., Bird, M. I., Korir, D. K., Levin, N. E., Mace,
789 W., Maccharia, A. N., Quade, J., and Remien, C. H.: Woody cover and hominin
790 environments in the past 6 million years, Nature, 476, 51-56, 2011.
791 Ciais, P., Friedlingstein, P., Schimel, D. S., and Tans, P. P.: A global calculation of
792 the δ13C of soil respired carbon: Implications for the biospheric uptake of
793 anthropogenic CO2, Global Biogeochemical Cycles, 13, 519-530, 1999.
794 Ciais, P., Cuntz, M., Scholze, M., Mouillot, F., Peylin, P., and Gitz, V.: Remarks on the
795 use of 13C and 18O isotopes in atmospheric CO2 to quantify biospheric
796 carbon fluxes, in: Stable Isotopes and Biosphere Atmosphere Interactions,
797 Academic Press, San Diego, CA, 235–267, 2005.
798 Clark, J.S.: Particle motion and the theory of charcoal analysis: source area,
799 transport, deposition and sampling, Quaternary Research, 30, 67–80, 1988.
800 Conedera, M., Tinner, W., Neff, C., Meurer, M., Dickens, A. F., and Krebs, P.:
801 Reconstructing past fire regimes: methods, applications, and relevance to
802 fire management and conservation, Quaternary Science Reviews, 28, 555-
803 576, 2009.
804 Cope, M. J., and Chaloner, W. G.: Fossil charcoal as evidence of past atmospheric
805 composition, Nature, 283, 647-649, 1980.
806 Das, O., Wang, Y., and Hsieh, Y.-P.: Chemical and carbon isotope characteristics of
807 ash and smoke derived from burning of C3 and C4 grasses, Organic
808 Geochemistry, 41, 263-269, 2010.
809 Dittmar, T.: The molecular level determination of black carbon in marine
810 dissolved organic matter, Organic Geochemistry, 39, 396-407, 2008.

Dittmar, T., de Rezende, C. E., Manecki, M., Niggemann, J., Ovalle, A. R. C., Stubbins, A., and Bernardes, M. C.: Continuous flux of dissolved black carbon from a vanished tropical forest biome, Nature Geoscience, 5, 618-622, 2012.

Domingues, T. F., Meir, P., Feldpausch, T. R., Saiz, G., Veenendaal, E. M., Schrodt, F., Bird, M. I., Djagbletey, G., Hien, F., Compaore, H., Diallo, A., Grace, J., and Lloyd, J.: Co-limitation of photosynthetic capacity by nitrogen and phosphorus along a precipitation gradient in West Africa, Plant, Cell and Environment, 33, 959-980, 2010.

Dümig, A., Rumpel C., Dignac M.-F., and Kögel-Knabner I.: The role of lignin for the δ13C signature in C_4 grassland and C_3 forest soils, Soil Biology and Biochemistry, 57, 1-13 2013.

Enting, I. G., Trudinger, C. M., and Francey, R. J.: A synthesis inversion of the concentration and d13C of atmospheric CO2, Tellus B, 47, 35-52, 1995.

Forbes, M. S., Raison, R. J., and Skjemstad, J. O.: Formation, transformation and transport of black carbon (charcoal) in terrestrial and aquatic ecosystems, Science of the Total Environment, 370, 190-206, 2006.

Furley, P. A., Rees, R. M., Ryan, C. M., and Saiz, G.: Savanna burning and the assessment of long-term fire experiments with particular reference to Zimbabwe, Prog. Phys. Geogr., 32, 611–634, 2008.

Haberle, S.: A 23,000-yr pollen record from Lake Euramoo, Wet Tropics of NE Queensland, Australia, Quaternary Research, 64, 343-356, 2005.

Hammes, K., Schmidt, M. W., Smernik, R. J., Currie, L. A., Ball, W. P., Nguyen, T. H., Louchouarn, P., Houel, S., Gustafsson, Ö., Elmquist, M., Cornelissen, G., Skjemstad, J. O., Masiello, C. A., Song, J., Peng, P., Mitra, S., Dunn, J. C., Hatcher, P. G., Hockaday, W. C., Smith, D. M., Hartkopf-Fröder, C., Böhmer, A., Lüer, B., Huebert, B. J., W., A., Brodowski, S., Huang, L., Zhang, W., Gschwend, P. M., Flores-Cervantes, D. X., Largeau, C., Rouzaud, J.-N., Rumpel, C., Guggenberger, G., Kaiser, K., Rodionov, A., Gonzalez-Vila, F. J., Gonzalez-Perex, J. A., de la Rosa, J. M., D.A.C., M., López-Capél, E., and Ding, L.: Comparison of quantification methods to measure fire-derived (black/elemental) carbon in soils and sediments using reference materials from soil, water, sediment and the atmosphere, Global Biogeochemical Cycles, 21, 2007.

Hartford, R. A., and Frandsen, W. H.: When it's hot, it's hot... or maybe it's not! (Surface flaming may not portend extensive soil heating). Int J Wildland Fire, 2, 139–144, 1992.

Keppler, F., Kalin, R. M., Harper, D. B., McRoberts W.C., and Hamilton J.T.G.: Carbon isotope anomaly in the major plant C_1 pool and its global biogeochemical implications, Biogeosciences, 1, 123-131, 2004.

Krull, E. S., Skjemstad, J. O., Graetz, D., Grice, K., Dunning, W., Cook, G. D., and Parr, J. D.: 13C-depleted charcoal from C3 and C4 grasses and the role of occluded carbon in phytoliths., Organic Geochemistry, 34, 1337–1352, 2003.

Kuhlbusch, T. A. J., Andreae, M. O., Cachier, H., Goldammer, J. G., Lacaux, J. P., Shea, R., and Crutzen, P. J.: Black carbon formation by savanna fires: Measurements and implications for the global carbon cycle, Journal of Geophysical Research, 101, 23651-23623, 1996.

Lehmann, J., Skjemstad, J., Sohi, S., Carter, J., Barson, M., Falloon, P., Coleman, K., Woodbury, P., and Krull, E.: Australian climate–carbon cycle feedback reduced by soil black carbon, Nature Geoscience, 1, 832-883, 2008.

Lloyd, J., and Farquhar, G. D.: 13C discrimination during CO2 assimilation by the terrestrial biosphere, Oecologia, 99, 201-215, 1994.
Loo, S. V., and Koppejan, J.: Handbook of biomass combustion and co-firing, Twente University Press, Enschede, the Netherlands, 2002.
Major, J., Lehmann, J., Rondon, M., and Goodale, C.: Fate of soil-applied black carbon: downward migration, leaching and soil respiration, Global Change Biology, 16, 1366-1379, 2010.
Masiello, C. A., and Druffel, E. R. M.: Black carbon in deep-sea sediments, Science, 280, 1911-1913, 1998.
Masiello, C. A.: New directions in black carbon organic geochemistry, Marine Chemistry, 92, 201-213, 2004.
Meredith, W., Ascough, P. L., Bird, M. I., Large, D. J., Snape, C. E., Sun, Y., and Tilston, E. L.: Assessment of hydropyrolysis as a method for the quantification of black carbon using standard reference materials, Geochimica et Cosmochimica Acta, 97, 131-147, 2012.
Miranda, A. C., Sinátora, H., Oliveira, I. F., and Ferreira, B.: Soil and air temperatures during prescribed cerrado fires in Central Brazil, Journal of Tropical Ecology, 9, 313–320, 1993.
O'Leary, M. H.: Carbon isotopes in photosynthesis, Bioscience, 38, 328-336, 1988.
O'Malley, V., Burke, R. A., and Schlotzhauer, W. S.: Using GC-MS/Combustion/IRMS to determine the 13C/12C ratios of individual hydrocarbons produced from the combustion of biomass materials--applications to biomass burning, Organic Geochemistry, 27, 567-581, 1997.
Randerson, J. T., Van der Werf, G. R., Collatz, G. J., Giglio, L., Still, C. J., Kasibhatla, P., Miller, J. B., White, J. W. C., DeFries, R. S., and Kasischke, E. S.: Fire emissions from C3 and C4 vegetation and their influence on interannual variability of atmospheric CO2 and δ13CO2, Global Biogeochemical Cycles, 19, GB2019, doi 10.1029/2004GB002366, 2005.
Rumpel, C., Alexis, M., Chabbi, A., Chaplot, V., Rasse, D. P., Valentin, C., and Mariotti, A.: Black carbon contribution to soil organic matter composition in tropical sloping land under slash and burn agriculture, Geoderma, 130, 35-46, 2006.
Saiz, G., Bird, M. I., Domingues, T., Schrodt, F., Schwarz, M., Feldpausch, T. R., Veenendaal, E. M., Djagbletey, G., Hien, F., Compaore, H., Diallo, A., and Lloyd, J.: Variation in soil carbon stocks and their determinants across a precipitation gradient in West Africa, Global Change Biology, 18, 1670-1683, 2012.
Saiz, G., Goodrick, I., Wurster, C., Zimmermann, M., Nelson, P., and Bird M. I.: Charcoal re-combustion efficiency in tropical savannas, Geoderma, 219–220, 40–45, 2014.
Santín, C., Doerr, S. H., Preston, C., and Bryant, R.: International Journal of Wildland Fire, Consumption of residual pyrogenic carbon by wildfire, 22, 1072-1077, 2013.
Santín, C., Doerr, S. H., Preston, C. M., & González-Rodríguez, G. (2014). Pyrogenic organic matter production from wildfires: a missing sink in the global carbon cycle. Global Change Biology. DOI: 10.1111/gcb.12800.
Seiler, W., and Crutzen, P. J.: Estimates of gross and net fluxes of carbon between the biosphere and the atmosphere from biomass burning, Climatic Change, 2, 207-247, 1980.

908 Still, C. J., Berry, J. A., Collatz, G. J., and DeFries, R. S.: Global distribution of C3 and
909 C4 vegetation: carbon cycle implications, Global Biogeochemical Cycles, 17,
910 1006, 2003.
911 Thevenon, F., D., W., Bard, E., F.S., A., Beaufort, L., and Cachier, H.: Combining
912 charcoal and elemental black carbon analysis in sedimentary archives:
913 Implications for past fire regimes, the pyrogenic carbon cycle, and the
914 human–climate interactions, Global and Planetary Change, 72, 381-389,
915 2010.
916 Torello-Raventos, M., Feldpausch, T. R., Veenendaal, E. M., Schrodt, F., Saiz, G.,
917 Domingues, T., Djagbletey, G., Ford, A., Kemp, J., Marimon, B. S., Marimon, B.
918 H. J., Lenza, E., Ratter, J. A., Maracahipes, L., Sasaki, D., Sonké, B., Zapfack, L.,
919 Taedoumg, H., Villarroel, D., Schwarz, M., Quesada, C. A., Ishida, F. Y., Nardoto,
920 G. B., Affum-Baffoe, K., Arroyo, L., Bowman, D. M. J. S., Compaore, H., Davies,
921 K., Diallo, A., Fyllas, N. M., Gilpin, M., Hien, F., Johnson, M., Killeen, T. J.,
922 Metcalfe, D., Miranda, H. S., Steininger, J., Thomson, J., Sykora, K., Mougin, E.,
923 Hiernaux, P., Bird, M. I., Grace, J., Lewis, S. L., Phillips, O. L., and Lloyd, J.: On
924 the delineation of tropical vegetation types with an emphasis on
925 forest/savanna transitions, Plant Ecology & Diversity, 6, 101-137, 2013.
926 Trollope, W. S. W.: Fire in savanna, in Ecological Effects of Fire in South African
927 Ecosystems, in, edited by: Booysen, P. D. V., and Tainton, N. M., Springer-
928 Verlag, Berlin, Germany, 199–218, 1984.
929 van der Werf, G. R., Randerson, J. T., Giglio, L., Collatz, G. J., Mu, M., Kasibhatla, P. S.,
930 Morton, D. C., DeFries, R. S., Jin, Y., and van Leeuwen, T. T.: Global fire
931 emissions and the contribution of deforestation, savanna, forest, agricultural,
932 and peat fires (1997–2009), Atmos. Chem. Phys., 10, 11707-11735,
933 doi:10.5194/acp-10-11707-2010, 2010.
934 Werf, G. V., Randerson, J. T., Giglio, L., Collatz, G. J., Mu, M., Kasibhatla, P. S.,
935 Morton, D. C., DeFries, R. S., and Leeuwen, T. V.: Global fire emissions and the
936 contribution of deforestation, savanna, forest, agricultural, and peat fires
937 (1997–2009). Atmospheric Chemistry and Physics, 10, 11707-11735, 2010.
938 Wessel, P., Smith, W. H. F., Scharroo, R., Luis, J. F., and Wobbe, F.: Generic
939 Mapping Tools: Improved version released, EOS Trans. AGU, 409-410, 2013.
940 Wright, H. A., and Bailey, A. W.: Fire ecology, John Wiley & Sons, New York, 1982.
941 Wurster C., Lloyd J., Goodrick I., Saiz G., and Bird M. I.: Quantifying the abundance
942 and stable isotope composition of pyrogenic carbon using hydrogen
943 pyrolysis. Rapid Communications in Mass Spectrometry, 26, 2690-2696,
944 2012.
945 Wurster C. M., Saiz G., Schneider M. P. W., Schmidt M. W. I., and Bird M. I.:
946 Quantifying pyrogenic carbon from thermosequences of wood and grass
947 using hydrogen pyrolysis, Organic Geochemistry 62, 28-32, 2013.
948 Wynn, J. G., Bird, M. I., Vellen, L., Grand-Clement, E., Carter, J., and Berry, S. L.:
949 Continental-scale measurement of the soil organic carbon pool with climatic,
950 edaphic, and biotic controls, Global Biogeochemical Cycles, 20, GB1007, 2006.
951 Wynn, J. G., and Bird, M. I.: C4-derived soil organic carbon decomposes faster
952 than its C3 counterpart in mixed C3/C4 soils, Global Change Biology, 13,
953 2206-2217, 2007.
954 Wynn, J. G., and Bird, M. I.: Environmental controls on the stable carbon isotopic
955 composition of soil organic carbon: Implications for modelling the
956 distribution of C3 and C4 plants, Australia, Tellus B, 60, 604-621, 2008.

957 Zimmerman, A. R.: Abiotic and microbial oxidation of laboratory-produced black
958 carbon (biochar), Environmental science & technology, 44, 1295-1301, 2010.
959 Zimmermann, M., Bird, M. I., Wurster, C., Saiz, G., Goodrick, I., Barta, J., Capek, P.,
960 Santruckova, H., and Smernik, R.: Rapid degradation of pyrogenic carbon,
961 Global Change Biology, 18, 3306-3316, 2012.

962

963 **Table 1**: Characteristics of the studied sites.

Site	Latitude (°S)	Longitude (°E)	MAP (mm)	MAT (°C)	CC (%)
DCR (Davies Creek NP)	16.997	145.574	2050	21.3	55
BRK (Brooklyn Nature Refuge)	16.586	145.155	1650	22.5	40
UND (Undara NP)	18.208	144.658	795	23.6	30
MIT (Mitchell Grassland)	21.403	144.677	435	24.3	5

964 MAP = mean annual precipitation and MAT = mean annual temperature. Climate data
965 derives from the Australian Bureau of Meteorology. For the calculation of woody
966 canopy cover (CC) the reader is referred to Domingues et al. (2010).

967

Table 2: Mass balance of C fluxes in each of the fires.

Fire-Exp.	% Grass biomass	± 1/2 range	Max T (°C)	Resid. time (min)	pre-fire biomass TOC (g)	pre-fire ground TOC (g)	pre-fire ground HyPyC (g)	post-fire proximal PyC (g)	post-fire proximal HyPyC (g)	post-fire distal PyC (g)	post-fire distal HyPyC (g)	PyC/ TCE (%)	HyPyC/ TCE (%)	proximal/ total HyPyC	Post-fire CO_2 of combustion, mass-balance calculated (g C)
MIT 1 (G)	99.8	0	631	1.25	243.9	31.2	0.9	53.2	14.8	1	0.2	20	5	98	220.0
MIT 2 (G)	99.7	0.1	725	1.33	279	53.5	1.1	45	9.4	0.4	0.1	14	3	99	285.9
MIT 3 (T)	99	0.5	468	0.83	142.4	15	0.3	26.1	9.7	0.4	0.1	17	6	99	130.6
MIT 4 (T)	97.5	0.9	597	0.83	175.8	23	0.4	22.4	7.9	0.6	0.3	12	4	96	175.3
UND 1 (G)	88.3	0.6	676	1.58	271.3	116.9	9.5	58.8	24.1	0.3	0.1	15	4	100	319.6
UND 2 (G)	84.3	4.3	766	1.67	279.3	109.7	10.2	66.6	24.8	1.2	0.4	17	4	97	311.0
UND 3 (T)	57	6.1	500	1.58	239.8	94.2	10.6	55.7	14	0.6	0.1	17	1	97	267.1
UND 4 (T)	68.4	1.4	604	3.67	281.4	137.3	20.2	[1]na	[1]na	[1]na	[1]na	[1]na	[1]na	[1]na	[1]na
BRK 1 (T)	81.6	1.6	875	1.08	284	111.3	1.6	45.8	10.8	1.3	0.6	12	2	94	346.5
BRK 2 (T)	74.2	1.2	na	na	389.4	82.7	2.7	60.3	12	0.7	0.3	13	2	97	408.5
BRK 3 (G)	94.8	1	551	1.92	257.9	98.8	2.1	60.2	16.5	0.9	0.4	17	4	97	293.5
BRK 4 (G)	86.7	0.5	665	2	338.9	149.5	5.4	61.1	13.6	0.8	0.3	13	2	96	421.1
DCR 1 (T)	41	5.2	572	14.5	523.7	125.4	2.9	117.9	12.4	[2]na	[2]na	[2]na	[2]na	[2]na	[2]na
DCR 2 (T)	34.6	0.6	591	6.17	584.6	209.3	5.1	91.9	13.3	1.5	0.8	12	1	91	695.4
DCR 3 (G)	48.3	6.1	427	8.67	311.2	164.8	10.6	81.2	16.5	1.9	1	17	1	85	382.2
DCR 4 (G)	42.9	5.4	527	5.42	355.7	187.7	12.9	123.7	19.4	1.6	0.8	23	1	90	405.1
All fires median (range)	83.0 (65.2)	1.1 (6.1)	597 (448)	1.7 (13.7)	280.4 (442.2)	110.5 (194.3)	4.0 (19.8)	60.2 (101.3)	13.6 (17.0)	0.8 (1.6)	0.3 (0.9)	16.0 (11.5)	2.5 (4.9)	96.9 (14.1)	333.0 (135.9)

Total organic carbon (TOC) and HyPyC are determined from the mass of the material collected in the 1 m^2 burned area for each of the fractions, and their C content measured before and after the HyPy treatment. Non-HyPyC is further distinguished between TOC and PyC for OC measured before and after the fire respectively. Burning locations are indicated by (G) and (T) for 'Grass' and 'Tree' dominated localities respectively (see Materials and Methods). Particle size fractions of each sample were summed into: (A) pre-fire ground, i.e., material that was collected from the surface before the fire, (B) post-fire proximal, i.e. material that was collected from the soil surface after the fire, combined with the >125 µm fraction of material collected at the filter collected at the chimney outlet.

Notes: [1]Mass balance in this experimental burn was not possible as the extraction pipe accidentally detached from the structure during the fire. [2]Sample was contaminated during manipulation and storage.

Deleted: Table 1

Formatted: Width: 29.7 cm, Height: 20.99 cm, Header distance from edge: 1.25 cm, Footer distance from edge: 1.25 cm

Table 3: Stable isotopic composition ($\delta^{13}C$ values) of C fluxes from each of the fires; standard errors of the means are shown in parentheses. Explanations for the different fractions are as in Table 2.

Fire Exp.	pre-fire biomass TOC $\delta^{13}C$ (‰)	[1]pre-fire biomass mass-based $\delta^{13}C$ (‰)	pre-fire ground TOC $\delta^{13}C$ (‰)	[2]pre-fire measured TCE $\delta^{13}C$ (‰)	pre-fire ground HyPyC $\delta^{13}C$ (‰)	post-fire proximal PyC $\delta^{13}C$ (‰)	post-fire proximal HyPyC $\delta^{13}C$ (‰)	post-fire distal PyC $\delta^{13}C$ (‰)	post-fire distal HyPyC $\delta^{13}C$ (‰)	Post-fire CO_2 of combustion, mass-balance calculated (‰)
MIT 1 (G)	-14.5	-13.2	-16.7	-14.8	-13.9	-16.0	-14.8	-20.7	-15.9	-14.4
MIT 2 (G)	-14.3	-13.2	-16.6	-14.7	-15.2	-16.7	-16.4	-20.4	-20.1	-14.3
MIT 3 (T)	-14.4	-13.3	-16.9	-14.7	-15.8	-17.0	-15.5	-20.5	-20.1	-14.2
MIT 4 (T)	-14.7	-13.5	-18.1	-15.1	-16.2	-17.3	-15.5	-19.7	-19.6	-14.8
UND 1 (G)	-14.4	-14.8	-18.9	-15.7	-15.8	-18.7	-17.5	-20.8	-19.6	-15.2
UND 2 (G)	-15.1	-15.3	-19.1	-16.2	-15.9	-17.8	-16.7	-17.6	-16.9	-15.8
UND 3 (T)	-18.9	-19.2	-23.1	-20.2	-17.9	-21.6	-17.9	-20.8	-17.9	-19.9
UND 4 (T)	-15.7	-17.6	-23.9	-18.4	-17.9	-23.2	-17.7	-20.2	-18.8	[3]na
BRK 1 (T)	-14.8	-15.7	-21.9	-16.8	-21.2	-20.7	-16.5	-20.0	-19.1	-16.2
BRK 2 (T)	-16.3	-16.7	-18.0	-16.6	-22.3	-22.6	-18.5	-21.3	-19.8	-15.7
BRK 3 (G)	-13.1	-13.9	-18.0	-14.4	-20.0	-20.3	-16.4	-18.8	-18.8	-13.2
BRK 4 (G)	-14.1	-15.0	-21.5	-16.3	-21.9	-20.7	-16.8	-20.6	-19.8	-15.6
DCR 1 (T)	-22.2	-21.4	-25.4	-22.8	-24.3	-25.7	-23.0	[4]na	[4]na	[4]na
DCR 2 (T)	-22.2	-22.3	-25.9	-23.1	-25.4	-25.7	-22.9	-23.3	-23.5	-22.8
DCR 3 (G)	-17.8	-20.4	-25.7	-20.4	-24.7	-25.6	-23.9	-23.4	-23.1	-19.3
DCR 4 (G)	-21.3	-21.1	-25.6	-22.7	-25.4	-25.2	-22.4	-22.4	-22.1	-22.0
All Fires	-15.0 (9.1)	-15.5 (9.1)	-20.0 (9.0)	-16.5 (8.7)	-19.0 (11.5)	-20.7 (9.7)	-17.2 (9.1)	-20.6 (5.8)	-19.6 (7.6)	-15.7 (9.6)

Notes: [1]estimated carbon isotopic composition based on the mass of woody and grass biomass, assuming values for C_3 woody biomass (-27.2 ‰) and for C_4 grass biomass (-13.1‰); values from Cerling et al. (1997).
[2]TCE = total carbon exposed, mass-weighted isotopic composition of pre-fire biomass and ground TOC.
[3]Mass balance in this experimental burn was not possible as the extraction pipe accidentally detached from the structure during the fire. [4]Sample was contaminated during manipulation and storage.

Deleted: Table 2
Deleted: Table 1
Formatted: Left, None, Space Before: 0 pt, Don't keep with next, Don't keep lines together
Deleted: (-
Deleted: (-

Figures

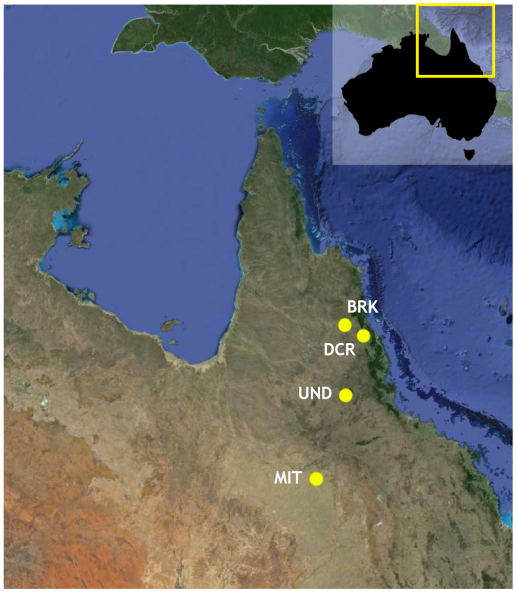

Figure 1: Geographical locations of the studied sites in northeast Australia. Source: "North East Australia" Image Landsat (2014) Google Earth.

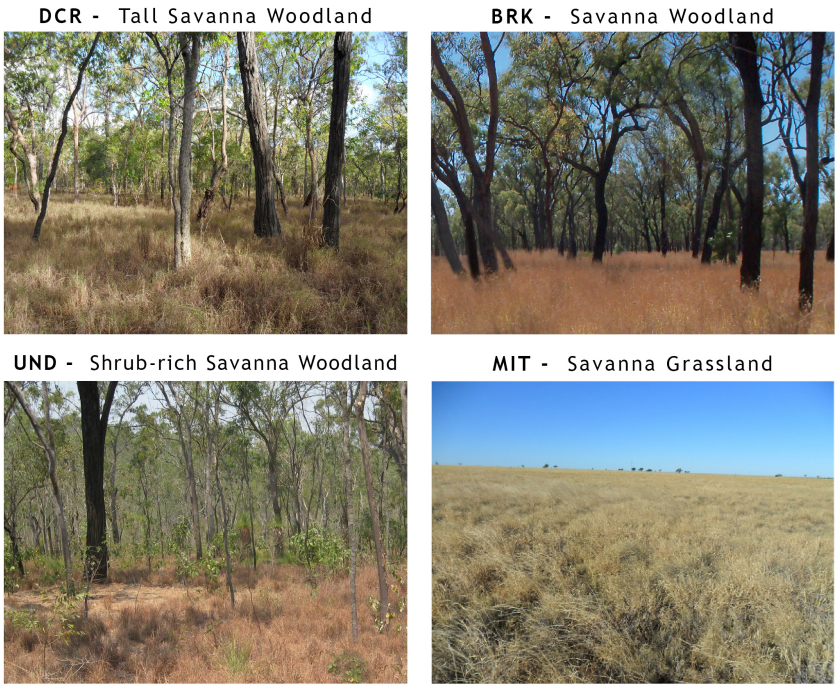

Site	MAP (mm)	MAT (°C)	CC (%)
DCR	2050	21.3	55
BRK	1650	22.5	40
UND	795	23.6	30
MIT	435	24.3	5

Figure 2: Characteristics and regional classification of the vegetation; the reader is referred to Torello-Raventos et al. (2013).

Deleted:

Formatted: Font:(Default) Times New Roman, Bold

Formatted: Font:(Default) Times New Roman

Deleted: Figure 1

Deleted: and locations of the studied sites. Geographical coordinates are given in latitude and longitude decimal degrees. MAP = mean annual precipitation and MAT = mean annual temperature. Climate data derives from the Australian Bureau of Meteorology. For the r

Deleted: and calculation of woody canopy cover (CC) the

Deleted: Domingues et al. (2010) and

Figure 3: Schematic diagram depicting an experimental burn, with pre- and post-fire C pools. Initial biomass and PyC inventory were quantified in the near vicinity of each planned burn location by means of destructively collecting all above-ground plant material and vacuuming the soil surface from two $1m^2$ census quadrats, as shown in left bottom picture.

Deleted: Figure 2

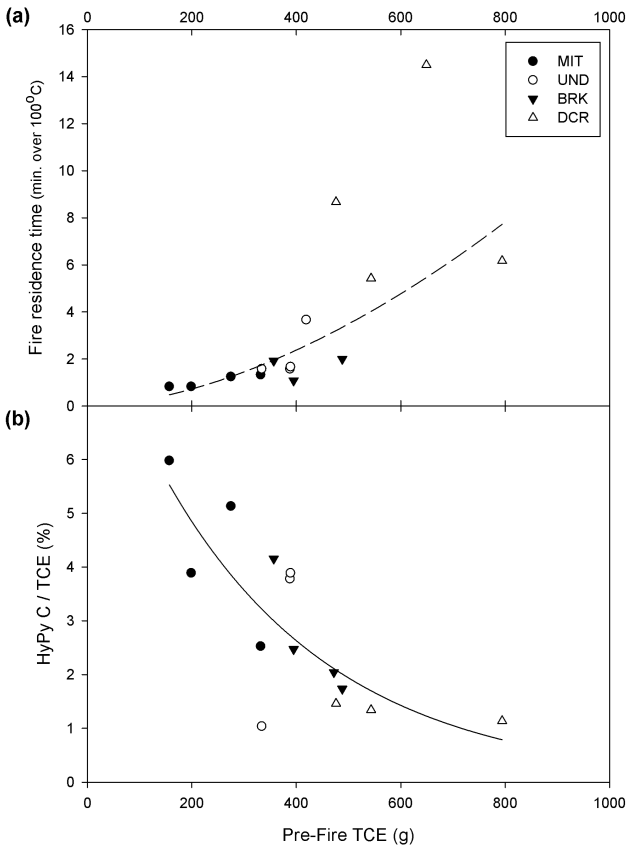

Figure 4: (a) Relationship between total carbon exposed (TCE) and fire residence time. The regression (dashed line) takes the following form: *Minutes over 100 ºC* $= 8 \times 10^{-5}$ *(TCE)*$^{1.719}$; r^2 *0.66;* $p < 0.05$; *BIC (Bayesian Information Criterion) 3.47; n=14.* (b) Relationship between TCE and the proportion of pyrogenic carbon produced (HyPyC) relative to TCE. The regression (solid black line) takes the following form: *HyPyC/ TCE (%) = 48.6 - 30.9 (TCE)*$^{0.066}$; r^2 *0.61;* $p < 0.05$; *BIC 6.27; n=14.* Different symbols group the individual burning experiments into the different ecosystems shown in Figure 2; individual data is presented in Table 2.

Deleted: Figure 3

Deleted: Figure 1

Deleted: Table 1

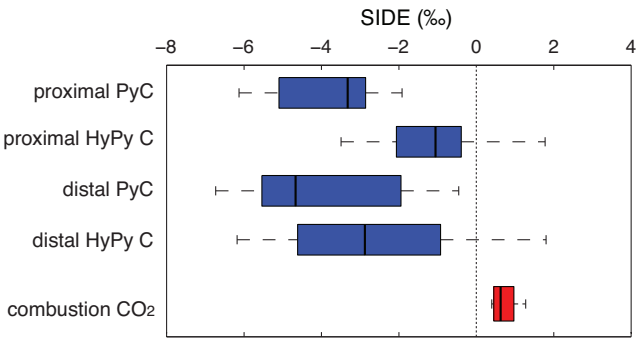

Figure 5: Box and whisker plot of isotopic disequilibrium values (SIDE = $\delta^{13}C_{flux}$– $\delta^{13}C_{pool}$) for proximal and distal fluxes of PyC and HyPyC, and combustion CO_2 calculated by mass-balance (n=16 for proximal components; n= 15 for distal components, n=14 for combustion CO_2). Line at centre of box represents the sample median, box represents 25th and 75th percentiles, and whiskers represent range.

Deleted: Figure 4

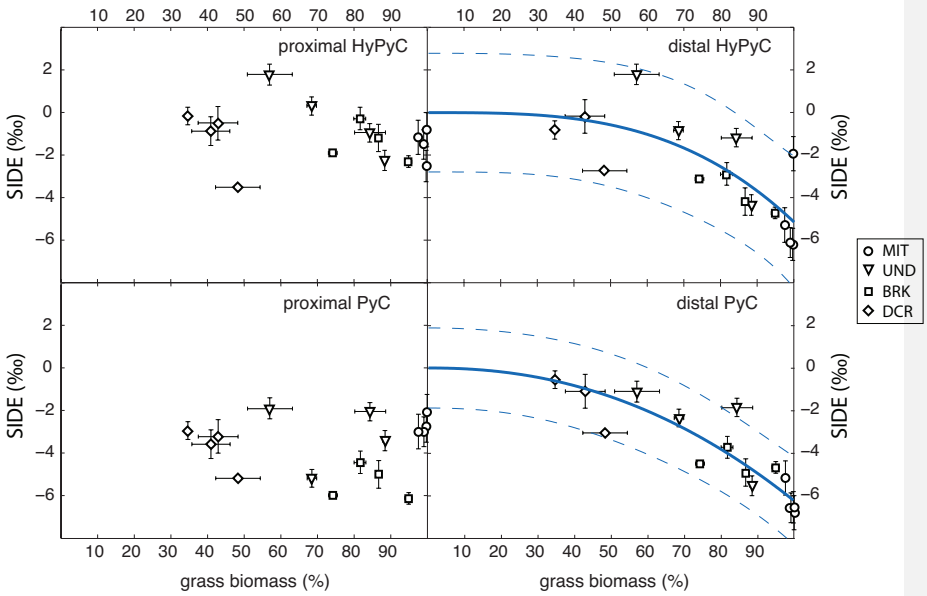

Figure 6: Relationship of isotopic disequilibrium values (SIDE = $\delta^{13}C_{flux}$–$\delta^{13}C_{pool}$) to the initial proportion of grass biomass (%, by mass). Error bars of % grass biomass represent the range of values measured from two 1 m^2 quadrats. Error bars of $\Delta\delta^{13}C$ represent values calculated using the difference from the isotopic composition of standing biomass ($\delta^{13}C_{pool}$) as determined by one of two methods: (1) measurement of the bulk C isotopic composition of biomass collected from the two quadrats, and (2) estimated carbon isotopic composition based on the mass of woody and grass biomass, assuming values for C_3 woody biomass (-27.2 ‰) and for C_4 grass biomass (-13.1‰; values from Cerling et al., 1997). Solid line shows best curve fit of power-law equation, with dashed lines representing 90% confidence intervals. n=16 for proximal components; n= 15 for distal components. Residuals of the power law fits to the distal HyPyC and distal PyC data showed a normal distribution (Jarque-Bera), with mean residual SIDE values of -0.03 and-0.02‰.

Deleted: Figure 5

Formatted: Indent: Left: 0 cm, Hanging: 0.5 cm, Line spacing: double

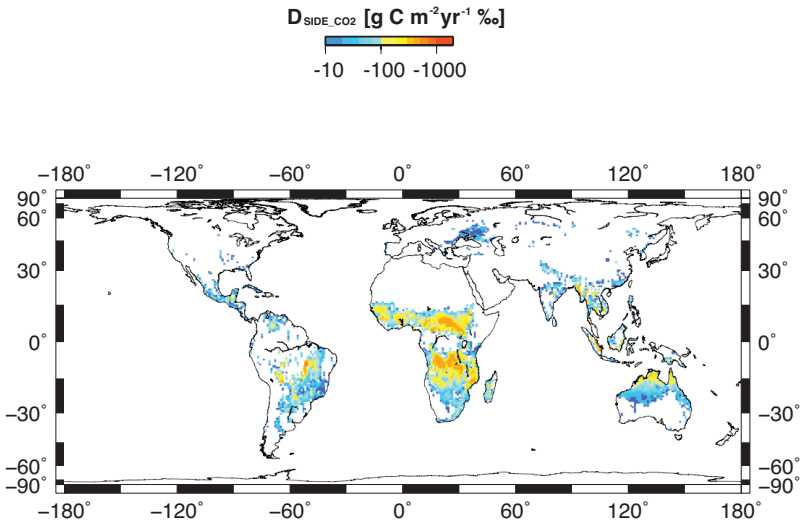

Figure 7: Global map of savanna isotope 'disequilibrium flux' (following terminology of Alden et al. (2010) $D_{SIDE\_CO2} = SIDE_{CO2} \times F_{bur}$) of the flux of CO_2 of combustion. The value of $SIDE_{CO2}$ used is 0.61‰. $F_{bur\text{-}savanna}$ is the mean annual flux of CO_2 from savanna fires, averaged over the period from 1997-2011 using the Global Fire Emissions Database (GFED; http://globalfiredata.org; van der Werf et al., 2010), clipped to the area where C_4 grasses > 1% (Still et al., 2003), with an estimated fraction of combusted CO_2 of 0.83 (estimated from Table 2).

Deleted: Figure 6

Deleted: Table 1